bioRxiv preprint doi: https://doi.org/10.1101/2020.07.06.189480; this version posted July 6, 2020. The copyright holder for this preprint (which was not certified by peer review) is the author/funder, who has granted bioRxiv a license to display the preprint in perpetuity. It is made available under aCC-BY-NC-ND 4.0 International license.

Global analysis of transcription start sites in the new ovine reference genome (*Oar rambouillet v1.0*)

Mazdak Salavati[1*], Alex Caulton[2,3*], Richard Clark[4], Iveta Gazova[1,5], Timothy P. L. Smith[6], Kim C. Worley[7], Noelle E. Cockett[8], Alan L. Archibald[1], Shannon M. Clarke[2], Brenda M. Murdoch[9], Emily L. Clark[1§] and The Ovine FAANG Project Consortium

[1]The Roslin Institute and Royal (Dick) School of Veterinary Studies, The University of Edinburgh, Edinburgh, UK
[2]AgResearch, Invermay Agricultural Centre, Mosgiel, New Zealand
[3]University of Otago, Dunedin, New Zealand
[4]Genetics Core, Edinburgh Clinical Research Facility, The University of Edinburgh, Edinburgh, UK
[5]MRC Human Genetics Unit, The University of Edinburgh, Edinburgh, UK
[6]USDA, Agricultural Research Service, USMARC, Clay Center, Nebraska, USA
[7]Baylor College of Medicine, Houston, Texas, USA
[8]Utah State University, Logan, Utah, USA
[9]University of Idaho, Moscow, Idaho, USA

*These two authors contributed equally to the work
[§]Corresponding author: emily.clark@roslin.ed.ac.uk

bioRxiv preprint doi: https://doi.org/10.1101/2020.07.06.189480; this version posted July 6, 2020. The copyright holder for this preprint (which was not certified by peer review) is the author/funder, who has granted bioRxiv a license to display the preprint in perpetuity. It is made available under aCC-BY-NC-ND 4.0 International license.

Abstract

The overall aim of the Ovine FAANG project is to provide a comprehensive annotation of the new highly contiguous sheep reference genome sequence (*Oar rambouillet v1.0)*. Mapping of transcription start sites (TSS) is a key first step in understanding transcript regulation and diversity. Using 56 tissue samples collected from the reference ewe Benz2616 we have performed a global analysis of TSS and TSS-Enhancer clusters using Cap Analysis Gene Expression (CAGE) sequencing. CAGE measures RNA expression by 5' cap-trapping and has been specifically designed to allow the characterization of TSS within promoters to single-nucleotide resolution. We have adapted an analysis pipeline that uses TagDust2 for clean-up and trimming, Bowtie2 for mapping, CAGEfightR for clustering and the Integrative Genomics Viewer (IGV) for visualization. Mapping of CAGE tags indicated that the expression levels of CAGE tag clusters varied across tissues. Expression profiles across tissues were validated using corresponding polyA+ mRNA-Seq data from the same samples. After removal of CAGE tags with < 10 read counts, 39.3% of TSS overlapped with 5' ends of transcripts, as annotated previously by NCBI. A further 14.7% mapped to within 50bp of annotated promoter regions. Intersecting these predicted TSS regions with annotated promoter regions (±50bp) revealed 46% of the predicted TSS were 'novel' and previously un-annotated. Using whole genome bisulphite sequencing data from the same tissues we were able to determine that a proportion of these 'novel' TSS were hypo-methylated (32.2%) indicating that they are likely to be reproducible rather than 'noise'. This global analysis of TSS in sheep will significantly enhance the annotation of gene models in the new ovine reference assembly. Our analyses provide one of the highest resolution annotations of transcript regulation and diversity in a livestock species to date.

Key words: Ovine, TSS, CAGE-Seq, WGBS, promotor, enhancer, RNA, transcriptome, FAANG, methylation, mRNA-Seq

bioRxiv preprint doi: https://doi.org/10.1101/2020.07.06.189480; this version posted July 6, 2020. The copyright holder for this preprint (which was not certified by peer review) is the author/funder, who has granted bioRxiv a license to display the preprint in perpetuity. It is made available under aCC-BY-NC-ND 4.0 International license.

Introduction

The Functional Annotation of Animal Genomes (FAANG) consortium is a concerted international effort to use molecular assays, developed during the Human ENCODE project (Birney et al., 2007), to annotate the majority of functional elements in the genomes of domesticated animals (Andersson et al., 2015; Giuffra and Tuggle, 2019). Towards this aim the overarching goal of the Ovine FAANG project (Murdoch, 2019) is to provide a comprehensive annotation of the new highly contiguous reference genome for sheep, *Oar rambouillet v1.0* (https://www.ncbi.nlm.nih.gov/assembly/GCF_002742125.1/). The Ovine FAANG project is developing a deep and robust dataset of expressed elements and regulatory features in the sheep genome as a resource for the livestock genomics community. Here we describe a global analysis of transcription start sites (TSS) using Cap Analysis Gene Expression (CAGE) sequencing.

CAGE measures RNA expression by 5' cap-trapping to identify the 5' ends of non-polyadenylated RNAs including lncRNAs and miRNAs, and has been specifically designed to allow the characterization of TSS within promoters to single-nucleotide resolution (Takahashi et al., 2012). This level of resolution allows investigation of the regulatory inputs driving transcript expression, and construction of transcriptional networks to study, for example, the genetic basis for disease susceptibility (Baillie et al., 2017) or for systematic analysis of transcription start sites through development (Lizio et al., 2017). Using CAGE sequencing technology, the FANTOM5 consortium generated a comprehensive annotation of TSS for the human genome, which included the major primary cell and tissue types (Forrest et al., 2014).

The goal of this study was to generate a comprehensive annotation of TSS and TSS-Enhancer clusters for the ovine genome. Our approach was to perform CAGE analysis on 55 tissues and one type of primary immune cell (alveolar macrophages). Tissues representing all the major organ systems were collected from Benz2616, the Rambouillet ewe used to generate the *Oar rambouillet v1.0* reference assembly. CAGE tags for each tissue sample clustered with a high level of specificity according to their expression profiles as measured by RNA-Seq. Mapping of CAGE tags indicated that a large proportion of detected TSS did not overlap with the current annotated 5' end of transcripts. The reproducibility of these 'novel' TSS was tested using whole genome DNA methylation profiles from a subset of the same tissues.

DNA methylation plays a key role in the regulation of gene expression and the maintenance of genome stability (Ibeagha-Awemu and Zhao, 2015), and is the most highly studied epigenetic mark. In mammalian species, DNA methylation occurs

bioRxiv preprint doi: https://doi.org/10.1101/2020.07.06.189480; this version posted July 6, 2020. The copyright holder for this preprint (which was not certified by peer review) is the author/funder, who has granted bioRxiv a license to display the preprint in perpetuity. It is made available under aCC-BY-NC-ND 4.0 International license.

primarily at cytosine-phosphate-guanine dinucleotides (CpG) and to a lesser extent at CHH and CHG sites (where C = Cytosine; H = Adenine, Guanine, or Thymine; and G = Guanine) (An et al., 2018). Generally, DNA methylation in the promoter region of genes represses transcription, inhibiting elongation by transcriptional machinery. Methylation over TSS blocks transcription initiation; while, conversely, methylation within gene bodies stimulates elongation and influences alternative splicing of transcripts (Jones, 2012; Lev Maor et al., 2015; An et al., 2018). Using DNA methylation profiles, we were able to determine the proportion of 'novel' TSS in our dataset that were likely true signals of transcription initiation based on a hypo-methylated state rather than being an artefact of CAGE-sequencing.

We provide the annotation of TSS in the ovine genome as tracks in a genome browser via the Track Hub Registry and visualise these in the R package GViz, ensuring the data is accessible and useable to the livestock genomics community. The global analysis of TSS we present here will significantly enhance the annotation of gene models in the new ovine reference assembly demonstrating the utility of the datasets generated by the Ovine FAANG project and providing a foundation for future work.

Methods

Animals

Tissues were collected from an adult female Rambouillet sheep at the Utah Veterinary Diagnostic Laboratory on April 29, 2016. At the time of sample collection Benz2616 was approximately 6 years of age and after a thorough veterinary examination confirmed to be healthy. Benz 2616 was donated to the project by the USDA. Sample collection methods were planned and tested over 15 months in 2015 to 2016, a description of these is available via the FAANG Data Coordination Centre https://data.faang.org/api/fire_api/samples/USU_SOP_Ovine_Benz2616_Tissue_Collection_20160426.pdf .

Sample collection

Necropsy of Benz2616 was performed by a veterinarian to ensure proper identification of tissues, and a team of scientists on hand provided efficient and rapid transfer of tissue sections to containers which were snap frozen in liquid nitrogen prior to transfer to -80C for long-term storage. Alveolar macrophages were collected by bronchoalveolar lavage as described in (Cordier et al., 1990). Details of all 100 samples collected from Benz2616 are included in the BioSamples database under

bioRxiv preprint doi: https://doi.org/10.1101/2020.07.06.189480; this version posted July 6, 2020. The copyright holder for this preprint (which was not certified by peer review) is the author/funder, who has granted bioRxiv a license to display the preprint in perpetuity. It is made available under aCC-BY-NC-ND 4.0 International license.

submission GSB-7268, group accession number SAMEG329607 (https://www.ebi.ac.uk/biosamples/samples/SAMEG329607) and associated information is recorded according to FAANG metadata specifications (Harrison et al., 2018). The FAANG assays, as described below, were generated from a subset of tissues for CAGE (56 tissues), polyA+ mRNA-Seq (58 tissues) and WGBS (8 tissues) (Figure 1).

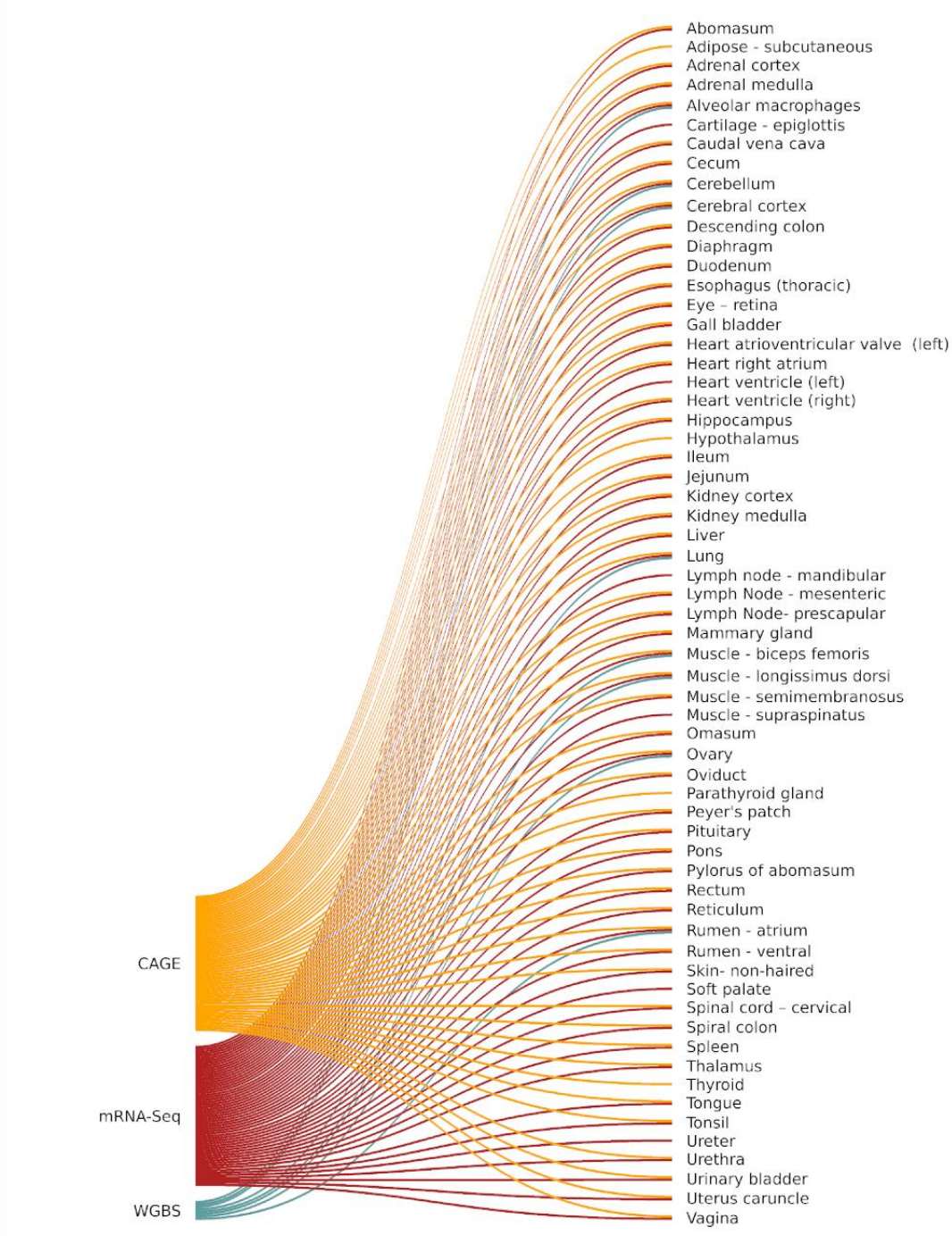

Figure 1. FAANG assays (CAGE, WGBS and mRNA-Seq) performed on each tissue from Benz2616.

bioRxiv preprint doi: https://doi.org/10.1101/2020.07.06.189480; this version posted July 6, 2020. The copyright holder for this preprint (which was not certified by peer review) is the author/funder, who has granted bioRxiv a license to display the preprint in perpetuity. It is made available under aCC-BY-NC-ND 4.0 International license.

CAGE Library Preparation and Analysis

RNA Isolation for CAGE library preparation

Frozen tissues (60-100mg per sample) were homogenised by grinding with a mortar and pestle on dry ice and RNA was isolated using TRIzol Reagent (Invitrogen) according to the manufacturer's instructions. After RNA isolation 10ug of RNA per sample was treated with DNase I (NEB) then column purified using a RNeasy MinElute kit (Qiagen), according to the manufacturer's instructions. Full details of the RNA extraction protocol are available via the FAANG Data Coordination Centre https://data.faang.org/api/fire_api/assays/USDA_SOP_RNA_Extraction_From_Tissue_20180626.pdf . Each RNA sample was run on an Agilent BioAnalyzer to ensure RNA integrity was sufficiently high (RIN^e>6). Details of RNA purity metrics for each sample are included in Supplementary Table 1. RNA samples were then stored at -80°C for downstream analysis.

CAGE library preparation and sequencing

CAGE libraries were prepared for each sample as described in (Takahashi et al., 2012) from a starting quantity of 5ug of DNase treated total RNA. Random primers were used to ensure conversion of all 5' cap-trapping RNAs according to (Takahashi et al., 2012). The full protocol is available via the FAANG Data Coordination Centre https://data.faang.org/api/fire_api/assays/ROSLIN_SOP_CAGE-library-preparation_20190903.pdf . Libraries were prepared in batches of eight and pooled. Sequencing was performed on the Illumina HiSeq 2500 platform by multiplexing 8 samples on one lane to generate approximately 20 million 50bp single-end reads per sample. Eight of the available fifteen 5' linker barcodes from (Takahashi et al., 2012) were used for multiplexing: ACG, GAT, CTT, ATG, GTA, GCC, TAG and TGG. In total 8 separate library pools were generated and spread across two HiSeq 2500 flow cells. Details of barcodes assigned to each sample and pool IDs are included in Supplementary Table 1.

Processing and mapping of CAGE libraries

All sequence data were processed using in house scripting (bash and R) on the University of Edinburgh high performance computing facility (Edinburgh, 2020). The analysis protocol for CAGE is available via https://data.faang.org/api/fire_api/analysis/ROSLIN_SOP_CAGE_analysis_pipeline_20191029.pdf and summarised in Figure 2. To de-multiplex the data we used the FastX toolkit version 0.014 (Hannon Lab, 2017) for short read pre-processing. We

bioRxiv preprint doi: https://doi.org/10.1101/2020.07.06.189480; this version posted July 6, 2020. The copyright holder for this preprint (which was not certified by peer review) is the author/funder, who has granted bioRxiv a license to display the preprint in perpetuity. It is made available under aCC-BY-NC-ND 4.0 International license.

then used TagDust2 v.2.33 (Lassmann, 2015) to extract mappable reads from the raw data and for read clean-up to remove the *EcoP1* site and barcode, according to the recommendations of the FANTOM5 consortium e.g. (Bertin et al., 2017). This process resulted in cleaned approximately 27bp reads (hereafter referred to as CAGE tags) which were mapped to the Rambouillet Benz2616 genome available from NCBI (*Oar rambouillet v1.0* GCA_002742125.1) using Bowtie2 v.2.3.5.1 in --very-sensitive mode equivalent to options *-D 20 -R 3 -N 0 -L 20 -i S,1,0.50* (Langmead and Salzberg, 2012). The mapped BAM files were then processed for base pair resolution strand specific read counts using bedtools v.2.29.0 (Quinlan and Hall, 2010). In order for the bedGraph files to be used in the CAGEfightR package they were converted to bigWig format using UCSCs tool BedGraphToBigWig (Kent et al., 2010).

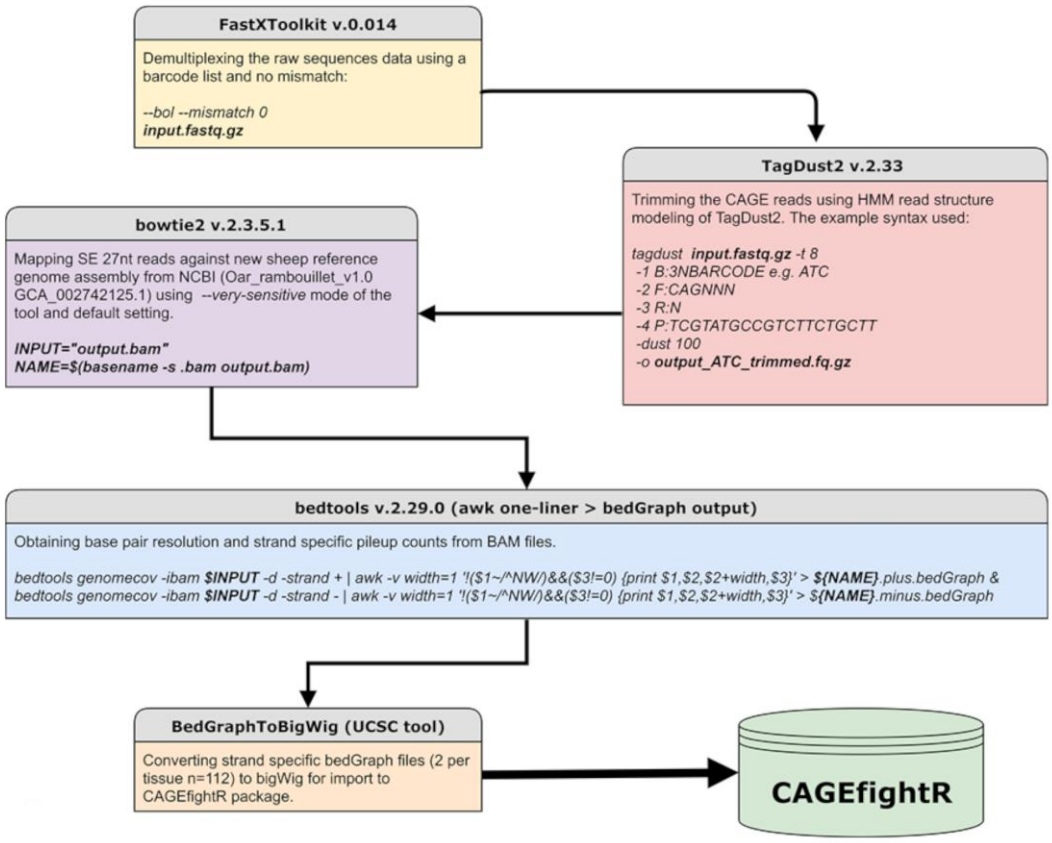

Figure 2. Workflow of the analysis pipeline and respective tools used for CAGE sequence data analysis

Normalisation and mapping of CAGE tags

For normalisation and clustering of CAGE tags (as CAGE Tags-Per-Million Mapped: CTPM) we used the software package CAGEfightR v.1.5.1 (Thodberg and Sandelin, 2019). The normalisation was performed via dividing CAGE tag counts in each

bioRxiv preprint doi: https://doi.org/10.1101/2020.07.06.189480; this version posted July 6, 2020. The copyright holder for this preprint (which was not certified by peer review) is the author/funder, who has granted bioRxiv a license to display the preprint in perpetuity. It is made available under aCC-BY-NC-ND 4.0 International license.

predicted cluster by the total mapped CAGE tags in the sample, multiplied by 1.0e6. To perform these analyses we created a custom BSgenome object (a container of the genomic sequence) for sheep from *Oar rambouillet v1.0* using the BSgenome Bioconductor package v.1.53.1 (Pages, 2020). Distribution metrics of CAGE tags across the genome were annotated and analysed using the TxDB transcript ID assignment and Genomic Features package v.1.36.4 (Lawrence et al., 2013). The TxDB object was created using the NCBI gff3 gene annotation file from NCBI *Oar rambouillet v1.0* GCA_002742125.1 (*GCF_002742125.1_Oar rambouillet v1.0 _genomic.gff release 103*).

Clustering of CAGE tags

To annotate TSS in the *Oar rambouillet v1.0* genome assembly we first generated expression read counts for each tag (bp resolution). Any tags with read counts < 10 (in each tissue) that were not present in at least 37/56 tissues (i.e. two thirds of the tissues) were removed. This conservative representation threshold was introduced to ensure CAGE tags included in downstream analysis were reproducible. In the absence of additional biological replicates we based this on the assumption that a CAGE tag was more likely to be reproducible if it was shared across multiple tissues, although sensitivity to putative highly tissue-specific TSS is reduced (see below). Gene annotation from the NCBI's GTF file was used to validate the coordinates of predicted CAGE clusters (i.e. residing within or outside the promoter of annotated genes). Five thresholds for representation, of CAGE tags across tissues, were compared (1 tissue, 1/3rd of the tissues, half of the tissues, 2/3rd of the tissues and all of the tissues). The proportion of CAGE tag clusters within (tagged by unique gene IDs) or outside the promoter region (untagged) was used to compare each threshold. Including all of the tissues (56/56 representation) resulted in 90.4% loss of genes tagged by any CAGE tag cluster i.e. only 2974 genes from a total of 30,862 genes in *Oar rambouillet v1.*0 were tagged by any CAGE tag cluster in the transcriptome. Reducing the threshold further to 1/3rd of tissues resulted in a high proportion of untagged CAGE tag clusters (40.9%) and 18,244 tagged genes. A less stringent reduction of the threshold to 2/3rd (37/56 tissues) resulted in 14,105 genes tagged by any CAGE tag cluster. The 2/3rd representation threshold was therefore chosen to maximise the number of annotated genes with expressed CAGE tags that were shared across tissues and minimise the number of CAGE tags mapped to outside the promoter region. Further details of this comparison are included in Supplementary File 1 Section 3. TSS expression profiles (as CTPM) were then generated for each tissue using the CAGEfightR v. 1.5.1 quickTSS, quickEnhancers and findLinks

bioRxiv preprint doi: https://doi.org/10.1101/2020.07.06.189480; this version posted July 6, 2020. The copyright holder for this preprint (which was not certified by peer review) is the author/funder, who has granted bioRxiv a license to display the preprint in perpetuity. It is made available under aCC-BY-NC-ND 4.0 International license.

functions (Thodberg and Sandelin, 2019). The CAGE tags clustered A) uni-directionally (according to the sense or anti-sense flag of the mapped CAGE tag) into predicted TSS and B) bi-directionally, using the TSS-Enhancer detection algorithm from CAGEfightR (Thodberg and Sandelin, 2019), into correlated TSS and enhancer (TSS-Enhancer) clusters. Bi-directional (TSS-Enhancer) clusters are defined as clusters of CAGE tags that are located on the opposing strand within 400 bp-1 Kbp proximity of the centre of a promoter (Thodberg and Sandelin, 2019). The bi-directional clusters outside of this range were excluded from this analysis according to the previously described method in (Thodberg et al., 2019). The concept of uni-directional and bi-directional clustering is illustrated in Figure 3.

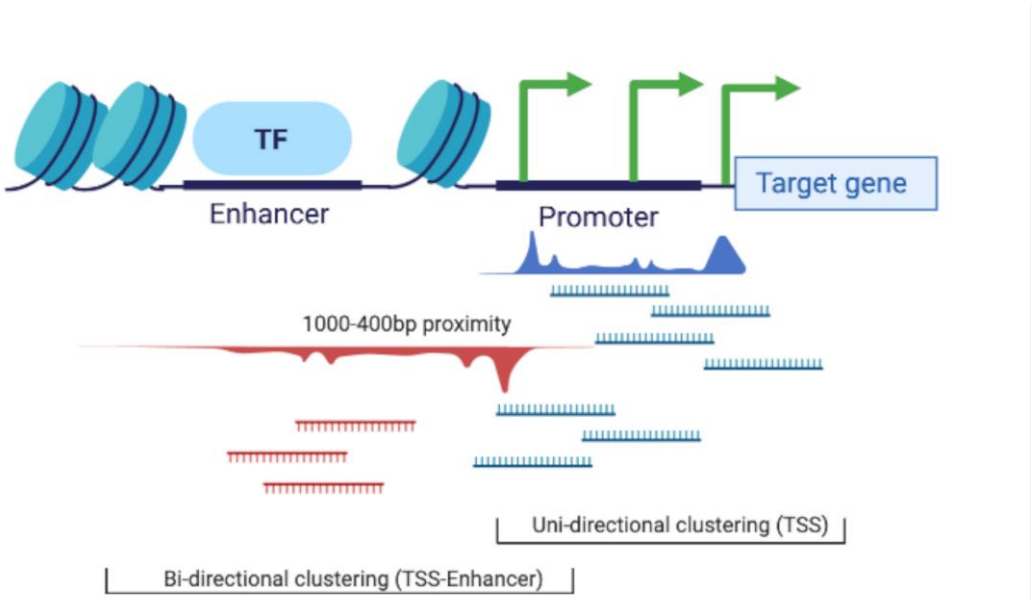

Figure 3. Schematic representation of the two clustering algorithms used in the CAGEfightR package for TSS (uni-directional) and TSS-Enhancer (bi-directional) clustering.

Identification of shared TSS or TSS-enhancer clusters across tissues

TSS or TSS-Enhancer clusters that were shared across tissues, were identified by investigating the CTPM expression profile of each of the tissues using correlation based and mutual information (MI) distance matrices (Priness et al., 2007; Reshef et al., 2018). This method of MI based clustering tolerates missingness and outlier-induced grouping errors in gene expression profiles (Priness et al., 2007). Using this method, we assumed that the CTPM expression profile, for each cluster, could vary across tissues, but for a predicted TSS or TSS-Enhancer cluster to be considered reproducible it must be present in at least two thirds of the tissues (37/56) in the dataset.

bioRxiv preprint doi: https://doi.org/10.1101/2020.07.06.189480; this version posted July 6, 2020. The copyright holder for this preprint (which was not certified by peer review) is the author/funder, who has granted bioRxiv a license to display the preprint in perpetuity. It is made available under aCC-BY-NC-ND 4.0 International license.

Identification of tissue-specific TSS or TSS-enhancer clusters

The 2/3rd representation threshold applied above would remove all tissue-specific CAGE tag clusters. To overcome this, a rerun of the clustering algorithm was performed with the representation threshold reduced. Tissue-specific uni-directional TSS clusters that were only present in 1/56 tissues were identified by filtering for CAGE tags with >10 expressed counts to create a data frame. The data frame was then filtered tissue-by-tissue to only retain uni-directional TSS clusters present in each tissue separately. This process was then repeated for the TSS-Enhancer clusters.

Annotation of 'novel' TSS in the ovine genome

We expected given the diversity of tissues sampled that we would detect a significant number of 'novel', previously unannotated TSS. The CAGE tag uni-directional clusters (TSS) were annotated using the mergeByOverlay function of the GenomicFeatures package in R and the custom TxDB object as following: *mergeByOverlaps(subject = TSS, query = promoters(txdb, upstream = 25, downstream = 25, use.names = T,c("tx_name", "GENEID")), maxgap = 25, type = "any").* The TxDB object calculates the range of the promoter based on the 5'UTR and first CDS codon coordinates. In each tissue any TSS region within 50bp range of the promoter coordinate of a gene model was considered 'annotated'. In addition, we expanded this range to 400bp to determine whether this would identify significantly more unannotated TSS further from the promoter. A reverse sub setting of the 50bp window region was performed as follows: *subsetByOverlaps(x = TSS ,ranges = annotated, invert = TRUE).* These regions were considered 'novel' TSS previously unannotated in the assembly. This process was repeated for every tissue separately (n=56).

Comparative analysis of WGBS and CAGE Data

Preparation of genomic DNA from tissue

Extraction of DNA for bisulphite sequencing was performed using phenol:chloroform:isoamyl alcohol method. Briefly, approximately 1 g frozen tissue was pulverized and resuspended in 2.26 ml of digestion buffer (10 mM Tris-HCl, 400 mM NaCl, 2 mM EDTA, pH 8.0) with 200 µl of SDS 10% and 60 µl RnaseA (10mg/ml) (Sigma-Aldrich, St. Louis, MO, USA) RNA degradation proceeded for one hour at 37ºC with gentle shaking. Next, 25 µl of proteinase K (20mg/ml) (Sigma-

bioRxiv preprint doi: https://doi.org/10.1101/2020.07.06.189480; this version posted July 6, 2020. The copyright holder for this preprint (which was not certified by peer review) is the author/funder, who has granted bioRxiv a license to display the preprint in perpetuity. It is made available under aCC-BY-NC-ND 4.0 International license.

Aldrich) was added to the suspension and incubated overnight (approximately 16 hours) at 37 °C with gentle shaking. The viscous lysate was transferred to a 2 mL Phase Lock tube (VWR, Radnor, PA) and extracted twice with Tris-HCl-saturated phenol:chloroform:isoamyl alcohol (25:24:1) pH 8.0, followed by extraction with 2.5 ml chloroform. The DNA was precipitated by addition of 5.5 ml of 100% ethanol and 250 µl of 3M Sodium Acetate to the aqueous phase in a 15 mL conical tube, mixed by gentle inversion until the DNA became visible. The DNA was removed with a bent Pastuer pipette hook, washed in 5 ml 70% cold ethanol, air dried then resuspended in 250 µl – 1 ml of 1X TE and stored at −20 °C until use. DNA concentration was quantified fluorometrically on the Qubit® 3.0 Fluorometer (Thermo Fisher Scientific, Waltham, MA, United States) using the Qubit dsDNA HS Assay Kit. The purity of the extractions was determined via 260/280 and 260/230 ratios measured on the NanoDrop 8000 (Thermo Fisher Scientific) and DNA integrity was assessed by 1% agarose gel electrophoresis. The protocol is available via the FAANG Data Coordination Centre https://data.faang.org/api/fire_api/assays/USDA_SOP_DNA_Extraction_From_Whole BloodandLiver_20200611.pdf.

Whole Genome Bisulphite Conversion and Sequencing

Library preparation and sequencing of seven tissues and 1 cell type (Figure 1), selected to include a representative from all major organ systems, were performed by The Garvan Institute of Medical Research, Darlinghurst, Sydney, New South Wales. Un-methylated lambda DNA was added at 0.5% of the total sample DNA concentration prior to bisulphite conversion as a conversion efficiency control. DNA conversion was carried out using the EZ DNA Methylation-Gold Kit (Zymo Research, CA, USA) following the manufacturer's instructions. The Accel-NGS Methyl-seq DNA kit (Swift Biosciences, MI, USA) for single indexing, was used to prepare the libraries, following the manufacturer's instructions. Libraries were pooled together and sequenced across 6 lanes of a flow-cell on an Illumina HiSeq X platform using paired end chemistry for 150 bp reads (min 10X coverage). The protocol is available via FAANG Data Coordination Centre https://data.faang.org/api/fire_api/assays/AGR_SOP_WGBS_AgR_Libary_prep_20200610.pdf

WGBS data processing

Paired end Illumina WGBS sequence data was processed and analysed using in house scripting (bash and R) and a range of purpose-built bioinformatics tools on the

bioRxiv preprint doi: https://doi.org/10.1101/2020.07.06.189480; this version posted July 6, 2020. The copyright holder for this preprint (which was not certified by peer review) is the author/funder, who has granted bioRxiv a license to display the preprint in perpetuity. It is made available under aCC-BY-NC-ND 4.0 International license.

AgResearch and University of Edinburgh high performance computing facilities. The analysis protocol for WGBS is available via the FAANG Data Coordination Centre https://data.faang.org/api/fire_api/analysis/AGR_SOP_WGBS_AgR_data_analysis_20200610.pdf and summarised below.

Briefly, FASTQ files for each sample, run across multiple lanes were merged together. TrimGalore v. 0.5.0. (https://github.com/FelixKrueger/TrimGalore) was used to trim raw reads to remove adapter oligos, poor quality bases (phred score less than 20) and the low complexity sequence tag introduced during Accel-NGS Methyl-seq DNA kit library preparation as follows: *trim_galore -q 20 --fastqc --paired --clip_R2 18 --three_prime_clip_R1 18 --retain_unpaired –o Trim_out INPUT_R1.fq.gz INPUT_R2.fq.gz*

A bisulphite-sequencing amenable reference genome was built using the *Oar rambouillet v1.0* , GenBank Accession number: GCA_002742125.1 genome with the BSSeeker2 script *bs_seeker2-build.py* using bowtie v2.3.4.3 (Langmead and Salzberg, 2012). and default parameters. The Enterobacteria phage lambda genome available from NCBI (Accession number: NC_001416) was added to the Oar_rambouillet *v1.0* genome as an extra chromosome to enable alignment of the unmethylated lambda DNA conversion control reads. Paired-end, trimmed reads were aligned to the reference genome using the BSSeeker2 script *bs_seeker2-align.py* and bowtie v2.3.4.3 (Langmead and Salzberg, 2012) allowing four mismatches (-m 4). Aligned bam files were sorted with samtools v1.6 (Li et al., 2009) and duplicate reads were removed with picard tools v2.17.11 (https://broadinstitute.github.io/picard/) MarkDuplicates function.

Deduplicated bam files were used to call DNA methylation levels using the “bam2cgmap” function within CGmaptools (Guo et al., 2018) with default options to generate ATCGmap and CGmap files for each sample. The ATCGmap file format summarises mapping information for all covered nucleotides on both strands, and is specifically designed for BS-seq data; whilst the CGmap format is a more condensed summary providing sequence context and estimated methylation levels at any covered cytosine in the reference genome.

Hyper-methylated and hypo-methylated regions were determined for each sample using methpipe v3.4.3 (Song et al., 2013). Specifically, CGmap files for each sample were reformatted for the methpipe v3.4.3 workflow using custom awk scripts. The methpipe symmetric-cpgs program was used to merge individual methylation levels at symmetric CpG pairs. Hypo-methylated and hyper-methylated regions were determined using the hmr program within methpipe, which uses a hidden Markov

bioRxiv preprint doi: https://doi.org/10.1101/2020.07.06.189480; this version posted July 6, 2020. The copyright holder for this preprint (which was not certified by peer review) is the author/funder, who has granted bioRxiv a license to display the preprint in perpetuity. It is made available under aCC-BY-NC-ND 4.0 International license.

model (HMM) using a Beta-Binomial distribution to describe methylation levels at individual CpG sites, accounting for the read coverage at each site.

Visualisation of the individual CpG site methylation levels with a minimum read depth cut-off of 10x coverage was done using Gviz package v.1.28.3 (Hahne and Ivanek, 2016).

Comparative analysis of annotated and 'novel' TSS with WGBS methylation information

We expected that reproducible TSS, either annotated or novel, would overlap with hypo-methylated regions of the genome (Yamashita et al., 2005; Yagi et al., 2008). To test whether this was true for those identified in our analysis, both annotated and novel TSS from the CAGE BED tracks were intersected with WGBS hypo methylation profiles using bedtools v.2.29.2 (Quinlan and Hall, 2010) and the following script: *bedtools intersect -b WGBS_HypoCpG.bed -a Novel_or_ Annotated.bed > Novel_or_annotated_HypoCpG.bed.* Any annotated and novel TSS (within a ±50bp window of the promoter) that intersected hypomethylated regions of DNA in each tissue, were verified as reproducible TSS and the remainder as 'noise'. The overlay of these regions was visualised as a genomic track using the Gviz package v.1.28.3 (Hahne and Ivanek, 2016).

Visualisation of the annotated TSS, mRNA-Seq and WGBS tracks in the ovine genome

In order to confirm the simultaneous expression of mRNA, CAGE tags corresponding to an active TSS and a hypomethylated region of DNA, a genomic track on which all three datasets could be visualised was generated. This visualisation consists of the following tracks: 1) Uni-directional CAGE tag clusters (TSS) 2) Bi-directional CAGE tag clusters (TSS-Enhancers) 3) WGBS hypomethylation score (bp resolution) 4) Transcript level expression (mRNA-Seq [TPM]) 5) The transcript models and 6) The gene model. Areas of the genome where TSS or TSS-Enhancer regions overlapped regions with a high hypomethylation score, within 5' end of an actively expressing transcript (TPM score), were considered reproducible TSS for that tissue. This process was performed using eight tissues with matching mRNA-Seq, CAGE and WGBS sequence data. The Gviz package v.1.28.3 was used to visualise these tracks (Hahne and Ivanek, 2016).

Validation of tissue-specific expression profiles

bioRxiv preprint doi: https://doi.org/10.1101/2020.07.06.189480; this version posted July 6, 2020. The copyright holder for this preprint (which was not certified by peer review) is the author/funder, who has granted bioRxiv a license to display the preprint in perpetuity. It is made available under aCC-BY-NC-ND 4.0 International license.

mRNA-Sequencing

Total RNA for mRNA-Seq from 32 tissues (Figure 1) was prepared, as above for the CAGE samples, by USMARC, and for 26 tissues by Baylor College of Medicine (BCM) using the MagMAX mirVana total RNA isolation kit (Thermo Fisher Scientific, Waltham, MA, United States) according to the manufacturer's instructions. Paired end polyA selected mRNA-Seq libraries were prepared and sequenced on an Illumina NextSeq500 at USMARC or the Ilumina HiSeq2000 at BCM using the Illumina Tru-Seq Stranded mRNA Library Preparation Kit. For each tissue a set of expression estimates, as transcripts per million (TPM), were obtained using the transcript quantification tool Kallisto v0.43.0 (Bray et al., 2016). The mRNA-Seq analysis pipeline is accessible via the FAANG Data Coordination Centre https://data.faang.org/api/fire_api/analysis/ROSLIN_SOP_RNA-Seq_analysis_pipeline_20200610.pdf. A pairwise distance matrix (multiple correlation coefficient based) was produced using MI values for all tissues and a dendrogram of tissues was created in order to visualise grouping patterns of tissues with similar mRNA expression profiles, and for comparison with the CAGE dataset.

Comparative analysis of tissue-specific expression profiles using information from CAGE and mRNA-Seq

We assessed whether TSS expression profiles from the CAGE dataset were biologically meaningful using the mutual information (MI) sharing algorithm (Joe, 1989). Tissues with the same function and physiology should have similar TSS expression profiles. The CTPM expression level was binned (n=10) using the bioDist package v.1.56.0 (Ding et al., 2012) and mutual information (MI) for each pair of tissue samples was calculated as in (Joe 1989). :

$$\delta = (1 - \exp(-2 \times \delta))^{0.5}$$

$$MI\ distance = 1 - \delta$$

A pairwise distance matrix (multiple correlation coefficient based) was produced using MI values for all tissues and a dendrogram of tissues created to visualise grouping patterns of tissues with similar TSS expression profiles. If the expression profiles were meaningful then tissues with similar function and physiology would group together in clades within the dendrogram. These tissue specific groupings were then further validated by comparison with mRNA-Seq data for the same samples, using the MI sharing algorithm and dendrogram approach.

bioRxiv preprint doi: https://doi.org/10.1101/2020.07.06.189480; this version posted July 6, 2020. The copyright holder for this preprint (which was not certified by peer review) is the author/funder, who has granted bioRxiv a license to display the preprint in perpetuity. It is made available under aCC-BY-NC-ND 4.0 International license.

Results

Library size and annotation metrics

The mean CAGE library depth based on raw CAGE tags was 4,862,957 tags. Library depth varied across tissues. Tissues with low depth were not related to any specific barcodes and were evenly spread over the two sequencing runs (Supplemental Table S1), suggesting random variation rather than systematic differences due to specific barcodes or sequencing uns. The RIN^{e} values were also consistently >7 for all tissues with low counts, indicating RNA integrity was also unlikely to be affecting library depth. Differences in tag numbers are therefore more likely to relate to variation in efficiency between individual libraries or tissue-specific differences related to the physiology of the tissue.

CAGE tag clustering and annotation by genomic regions

We used a newly developed software package to annotate TSS in the Rambouillet Benz2616 genome (Thodberg and Sandelin, 2019; Thodberg et al., 2019) which clustered the CAGE tags as A) uni-directionally into predicted TSS or B) bi-directionally into correlated TSS and enhancer (TSS-Enhancer) clusters (Figure 3). The clustered CAGE tags were filtered to remove any clusters with a minimum expression level of <10 tag counts.

In order to reduce 'noise' for downstream analysis (i.e. large proportions of un-annotated CAGE tags that were likely to be spurious) we applied a conservative 2/3rd representation criteria, i.e. a minimum of 37/56 tissues had to express the tag cluster with >10 expressed counts. Application of 2/3rd representation criteria resulted in 28,148 uni-directional TSS clusters, from a total of 5,450,864, for downstream analysis. The mean (±SD) and median number of tissues per cluster was 3.68 ± 4.78 and 2, respectively. This level of noise in CAGE sequencing datasets (0.5% retained clusters) is somewhat lower than reported for other mammalian promoter-level expression atlas projects, e.g. by the FANTOM consortium, using less conservative criteria, where approximately 5% of clusters were retained (Forrest et al., 2014).

Bi-directional TSS-enhancer clusters were far fewer in number, although retention was higher with over 23% meeting the same 2/3rd representation criteria 741 from a total of 3,131. Though fewer in number these bi-directional (or TSS-enhancer) clusters are functionally important in the regulation of expression of their target genes (Andersson et al., 2014; Thodberg and Sandelin, 2019), consistent with finding them in over 2/3rd of tissues. The co-expression of leading enhancer RNA

bioRxiv preprint doi: https://doi.org/10.1101/2020.07.06.189480; this version posted July 6, 2020. The copyright holder for this preprint (which was not certified by peer review) is the author/funder, who has granted bioRxiv a license to display the preprint in perpetuity. It is made available under aCC-BY-NC-ND 4.0 International license.

(eRNA) which is captured by CAGE sequencing can provide a map to enhancer families in the genome and the genes under their regulation (Andersson et al., 2014).

The locations of both uni-directional TSS and bi-directional TSS-enhancer clusters were identified in *Oar rambouillet v1.0* and the proportion of TSS clusters located within or near annotated gene features was estimated (Figure 4). The custom BSgenome and TxDB objects created from the GFF3 file format provide detailed calculated coordinates for the following sections: intergenic (>1000bp before 5'UTR or after the end of 3'UTR), proximal (1000bp upstream of the 5'UTR), promoter (±100bp from 5'UTR) and the standard gene model (5'UTR, exon, intron and 3'UTR). The genomic region class with the highest number of unidirectional clusters (39.25%) was the promoter regions (±100bp from 5'UTR) (Figure 4A), with a relatively even distribution within the other regions of the genome, including 6% mapping proximally to the 5'UTR. The majority of bi-directional TSS-enhancer clusters were also located in promoter regions (70.1%) with a smaller proportion (25.6%) located in proximal regions (Figure 4B). The lack of bi-directional TSS-enhancer clusters in other regions is a consequence of the operation of the CAGEfightR algorithm, which only considers bi-directional clusters within a 400-1000bp window of a TSS CAGE tag cluster (Thodberg and Sandelin, 2019; Thodberg et al., 2019). This approach also reduced the total count compared to unidirectional clusters (28,148 uni-directional clusters relative to 741 bidirectional TSS-enhancer clusters across tissues) (Thodberg et al., 2019).

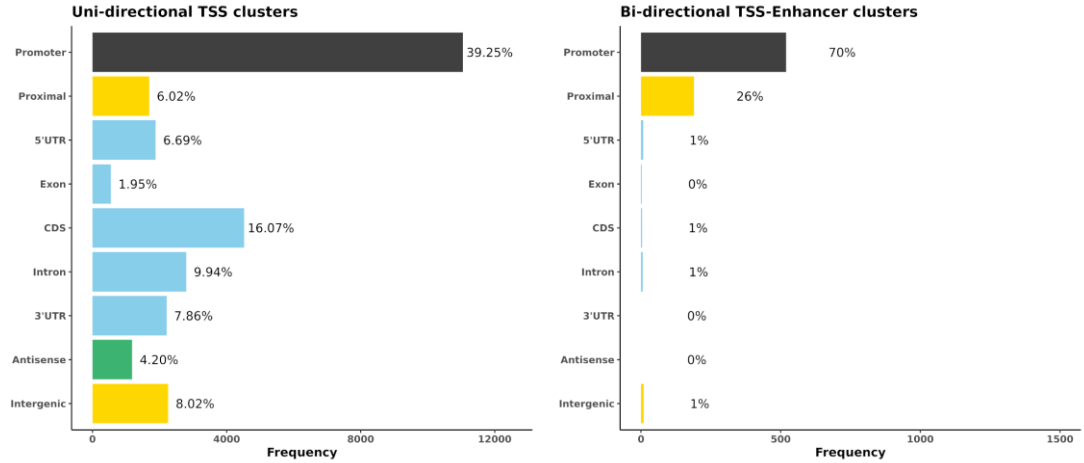

Figure 4. The genomic region distribution of CAGE tag clusters mapped against Oar rambouillet v1.0 assembly and gene annotation. The counts were averaged across tissues. A) Uni-directional TSS clusters with the highest proportion in promoter region (±100bp of the 5'UTR beginning at the [TSS]). B) Bi-directional TSS-enhancer clusters with the highest proportion in the proximal region (1000bp upstream of the 5'UTR beginning at the [TSS]).

bioRxiv preprint doi: https://doi.org/10.1101/2020.07.06.189480; this version posted July 6, 2020. The copyright holder for this preprint (which was not certified by peer review) is the author/funder, who has granted bioRxiv a license to display the preprint in perpetuity. It is made available under aCC-BY-NC-ND 4.0 International license.

Distribution of CAGE tag clusters in *Oar rambouillet v1.0* relative to *Oar_v3.1*

As a proxy for improvement in the accuracy of the gene models in *Oar rambouillet v1.0* we investigated how mapped CAGE tag clusters were distributed across genomic features when compared with *Oar_v3.1* (Jiang et al., 2014), the reference genome assembly it superseded (Supplemental Figure S2). The percentage of uni-directional CAGE tag clusters mapping to intergenic regions, which usually occurs due to missing gene model information, was greater for *Oar_v3.1* (33.9%) relative to *Oar rambouillet v1.0* (8%). The percentage of uni-directional CAGE tag clusters mapping to annotated promoter regions was greater for *Oar rambouillet v1.0* (39.25%) compared to *Oar_v3.1* (14.94%), indicating the proportion of accurate gene models in *Oar rambouillet v1.0* was greater. Ensembl annotated 20,921 protein coding genes, 5,843 non-coding genes and 29,118 transcripts on *Oar_v3.1*. NCBI annotated 20,883 protein-coding genes, 7,533 non-coding and 62,535 transcripts on *Oar rambouillet v1.0*. Of the 28,148 unidirectional TSS clusters mapped to *Oar rambouillet v1.0,* 87.74% mapped to 13,868 unique genes (31,729 transcripts). In comparison, of the 23,829 unidirectional TSS clusters mapped to *Oar_v3.1,* 49.1% mapped to 6,549 genes (9,914 transcripts). A larger number of TSS-Enhancer CAGE clusters were detected in *Oar_v3.1* (1121) in comparison to *Oar rambouillet v1.0* (741) mapping to 1371 and 2598 unique genes, respectively. A detailed comparison of mapping of the CAGE tags to the two reference assemblies is included in Supplementary File 1, Sections 1 and 2.

Mapping of CAGE tags shared across all tissue samples

Correlation-based and mutual information (MI) distance matrices were used to evaluate the occurrence of TSS and enhancer TSS across tissues. The mean ± SD number of tissues in which each cluster passing the 2/3rd criteria (expressed in 37/56 tissues) was (47.73 ± 6.03). Uni-directional TSS clusters (n=28,148 TSS regions) that were shared across tissues and detected in at least 37/56 tissues are visualised in Figure 5. Each chord in Figure 5 represents the presence of an expressed unidirectional TSS cluster shared across tissues. The majority of the unidirectional TSS that were shared across tissues mapped to promoters (39.25%) and were shared evenly across the tissues sampled (Figure 5). Some tissues e.g. mammary gland, pituitary gland and urinary bladder had more uni-directional TSS mapping to intergenic regions, which might indicate evidence of alternative splicing or differential TSS usage across tissues (Figure 5). Alternative splicing events and differential TSS usage, captured by CAGE, are often not included in the reference gene prediction models (Berger et al., 2019).

bioRxiv preprint doi: https://doi.org/10.1101/2020.07.06.189480; this version posted July 6, 2020. The copyright holder for this preprint (which was not certified by peer review) is the author/funder, who has granted bioRxiv a license to display the preprint in perpetuity. It is made available under aCC-BY-NC-ND 4.0 International license.

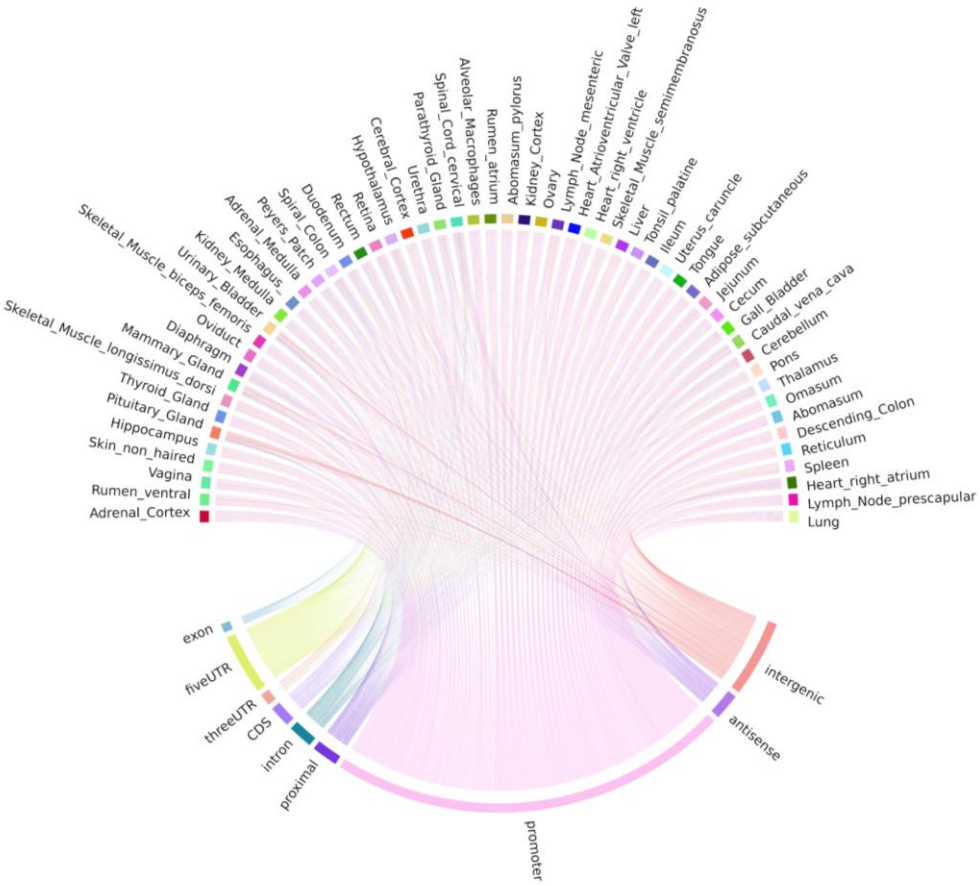

Figure 5. Chord diagram of expression level (TPM) of CAGE tag clusters (uni-directional TSS) across all the tissues collected from Benz2616. Shared CAGE tag clusters are common to at least 2/3rd of the tissues (37/56).

Bi-directional TSS-Enhancer CAGE clusters were far fewer in number but were shared in a similar pattern across tissues as the uni-directional TSS clusters (Figure 6). The majority (70.1%) of the TSS-Enhancer clusters mapped to promoters (n=520) while 25.6% mapped to 'proximal' regions as expected according to the 400bp-1Kbp detection window for TSS-Enhancer clusters from the centre of the promoter (Figure 6). For some tissues including abomasum, spleen and heart right atrium the proportion of bi-directional TSS-Enhancer clusters mapping to proximal regions was greater indicating more enhancer families could be present within these tissues (Figure 6).

bioRxiv preprint doi: https://doi.org/10.1101/2020.07.06.189480; this version posted July 6, 2020. The copyright holder for this preprint (which was not certified by peer review) is the author/funder, who has granted bioRxiv a license to display the preprint in perpetuity. It is made available under aCC-BY-NC-ND 4.0 International license.

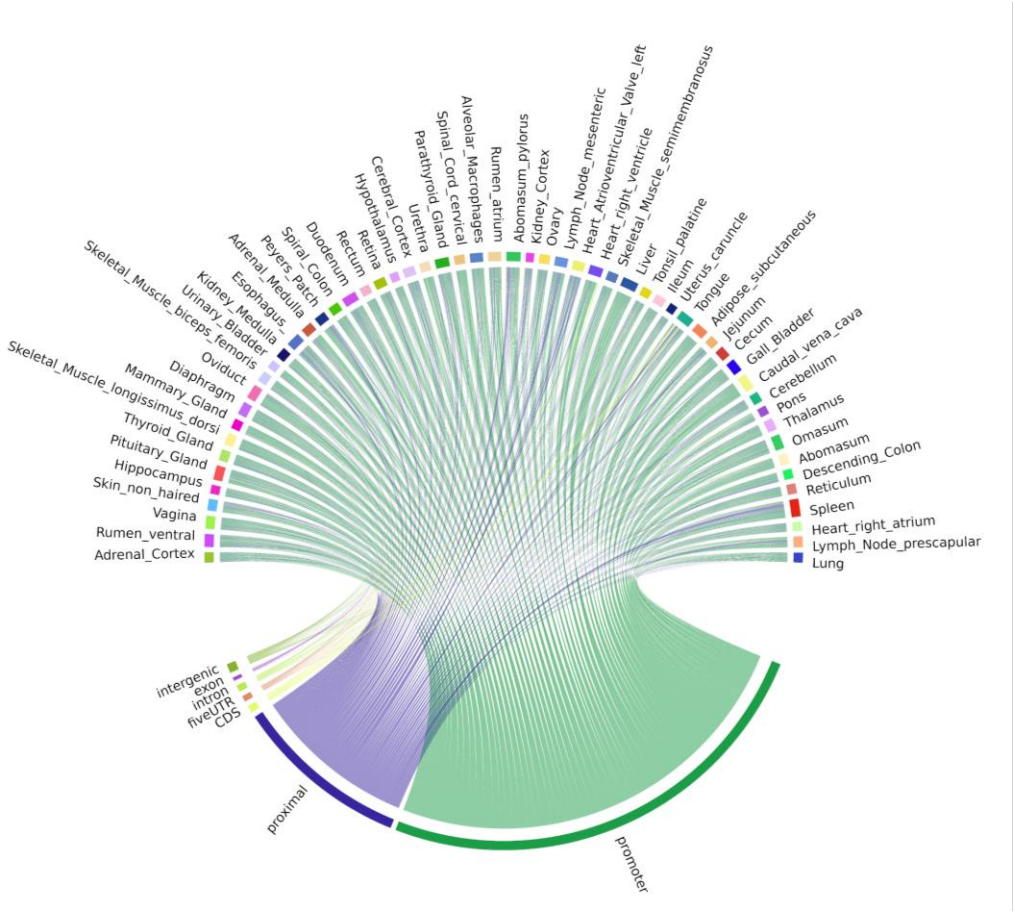

Figure 6. Chord diagram of expression level (TPM) of CAGE tag clusters (bi-directional TSS-Enhancer) across all the tissues collected from Benz2616. CAGE tag clusters expressed (>10 CTPM) by at least 2/3rd of the tissues (37/56).

Mapping of tissue-specific CAGE tags

The application of the 2/3rd criteria reduced the level of "noise" in assigning TSS and TSS enhancer elements, but eliminated the ability to observe potential tissue-specific CAGE tags or TSS clusters. Tissue-specific tags, i.e. those observed in only one of the 56 tissues, were examined to evaluate the ability to distinguish tissue-specific clusters from the background. A total of 3,228,425 tags were observed in only one tissue, and a much higher proportion (80.0%) of these tags mapped to intergenic and intronic regions compared to tags found across tissues, suggesting they do not represent true TSS (Supplementary Table 2). Only 0.8% of the tissue-specific CAGE tag clusters mapped to promoter or proximal regions (Supplementary Table 2). The caecum (n=1554), cerebellum (n=601) and longisimus dorsi muscle (n=477) had the highest number of tissues-specific predicted unidirectional TSS. The greatest number of expressed TSS (>1 CTPM) were detected in ceberellum (84/601) as shown in Supplementary Figure S3A. However, the expression level of tissue-specific CAGE

bioRxiv preprint doi: https://doi.org/10.1101/2020.07.06.189480; this version posted July 6, 2020. The copyright holder for this preprint (which was not certified by peer review) is the author/funder, who has granted bioRxiv a license to display the preprint in perpetuity. It is made available under aCC-BY-NC-ND 4.0 International license.

tag clusters was very low (<2 CTPM), which combined with the small sample size (n=1) for each tissue, meant that analysis of tissue-specific TSS was not particularly meaningful using this dataset. The analysis was repeated for tissue specific TSS-Enhancer clusters which is detailed in Supplementary Figure S3B.

Proportion of 'novel' TSS within the CAGE dataset for each tissue

CAGE tag clusters were annotated initially using the *Oar rambouillet v1.0* gene models from NCBI. A tissue-by-tissue annotation was performed using the same gene models to identify any CAGE tag clusters within a 50bp window of the promoter boundaries of every gene. From a total of 23,837 TSS (the average number of TSS per tissue) we found 11,328 (49.6%) were located within 50bp of the promoter. The CAGE tag clusters were annotated using the NCBI *Oar rambouillet v1.0* GFF3 gene track file (version 103) and a TxDB object created in the GenomicFeatures package (version 1.36.4) in R. CAGE tag clusters within 50bp (short range) or 400bp (long range) of the promoter were defined as annotated. Supplementary File 2 includes BED files for these CAGE tag clusters. The percentage of 'novel' previously un-annotated, but likely to be reproducible, CAGE tag clusters for each tissue within 50bp (short range) and 400bp (long range) from the promoter are detailed in Table 1.

Table 1: The total number and percentage of 'novel' CAGE tag clusters for each tissue within 50bp (short range) and 400bp (long range) from the promoter.

Tissue	*% Novel*	*Tags within 50bp*	*Tags within 400bp*	*Total*
Abomasum	49.38	8,161	8,688	16,584
Abomasum pylorus	49.89	12,339	13,074	25,963
Adipose subcutaneous	51.74	12,336	13,074	26,970
Adrenal cortex	51.79	12,285	13,019	26,859
Adrenal medulla	52.86	11,520	12,210	25,604
Alveolar macrophages	51.19	12,008	12,731	25,845
Caudal vena cava	37.75	10,937	11,578	18,179
Cecum	51.68	12,070	12,801	26,261
Cerebellum	48.59	8,393	8,936	16,796
Cerebral cortex	51.19	12,199	12,917	26,327
Descending colon	51.80	11,830	12,539	25,810
Diaphragm	52.53	10,367	11,016	22,733
Duodenum	52.34	11,243	11,932	24,620
Esophagus	49.90	10,016	10,625	20,741

bioRxiv preprint doi: https://doi.org/10.1101/2020.07.06.189480; this version posted July 6, 2020. The copyright holder for this preprint (which was not certified by peer review) is the author/funder, who has granted bioRxiv a license to display the preprint in perpetuity. It is made available under aCC-BY-NC-ND 4.0 International license.

Gall bladder	47.78	11,870	12,578	23,852
Heart atrioventricular valve left	50.90	12,268	13,000	26,330
Heart right atrium	52.96	10,996	11,666	24,444
Heart right ventricle	50.47	12,260	12,987	26,082
Hippocampus	53.40	12,142	12,878	27,451
Ileum	52.45	12,352	13,094	27,411
Jejunum	31.67	10,810	11,418	16,361
Kidney cortex	52.04	12,317	13,057	27,076
Kidney medulla	51.07	10,946	11,618	23,365
Liver	49.35	12,255	12,981	25,459
Lung	52.91	11,644	12,339	25,995
Lymph node mesenteric	46.34	12,132	12,838	23,742
Lymph node prescapular	53.56	11,533	12,228	26,096
Mammary gland	49.75	10,048	10,688	20,774
Omasum	39.89	9,167	9,708	15,692
Ovary	50.79	12,334	13,073	26,434
Oviduct	53.29	11,563	12,260	25,957
Payer's patch	52.41	11,881	12,578	26,240
Pituitary gland	47.25	6,918	7,362	13,400
Pons	40.69	11,622	12,296	20,506
Rectum	53.55	12,002	12,723	27,192
Reticulum	53.39	12,185	12,911	27,589
Retina	53.54	11,805	12,537	26,691
Rumen atrium	50.69	12,335	13,077	26,363
Rumen ventral	40.20	7,109	7,567	12,165
Skeletal muscle biceps femoris	50.23	12,151	12,872	25,715
Skeletal muscle longissimus dorsi	53.67	11,356	12,060	25,748
Skeletal Muscle semimembranosus	51.15	12,262	12,993	26,471
Spinal cord cervical	51.47	11,376	12,050	24,508
Spiral colon	53.25	11,937	12,662	26,813
Spleen	53.46	12,161	12,892	27,568
Thalamus	41.61	11,426	12,079	20,404
Tongue	39.57	9,639	10,244	16,512
Tonsil palatine	46.57	12,178	12,875	23,978
Urethra	52.76	11,387	12,087	25,292
Urinary bladder	51.68	11,163	11,840	24,174
Uterus caruncle	48.33	12,199	12,917	24,857
Vagina	52.30	11,600	12,300	25,543

bioRxiv preprint doi: https://doi.org/10.1101/2020.07.06.189480; this version posted July 6, 2020. The copyright holder for this preprint (which was not certified by peer review) is the author/funder, who has granted bioRxiv a license to display the preprint in perpetuity. It is made available under aCC-BY-NC-ND 4.0 International license.

Average	**49.60**	**11,328**	**12,009**	**23,837**

Comparative analysis of CAGE and WGBS to validate 'novel' TSS

True TSS and TSS enhancer elements are very likely to be associated with areas of hypomethylation (Yamashita et al., 2005, Yagi et al, 2008). The assessment of hypomethylation of regions where "novel" TSS were identified thus provides a means to support or refute their designation as true TSS. The methylation status of putative TSS regions for eight of the tissues used for CAGE analysis was examined at single nucleotide resolution using WGBS. Each WGBS library was pooled prior to sequencing and multiplexed across eight lanes of the HiSeq X 10 platform. Following trimming of the raw reads, the sequenced libraries produced an average of 103 Gbp of clean data. The average mapping rate of the reads was 78.8%. A small proportion (8.5%) of reads were identified as PCR or optical duplicates and were removed prior to downstream analysis. The average read depth of the filtered libraries was 20x coverage (Supplementary Table S3). Only cytosines with a minimum of ten reads were retained for the subsequent comparative analysis with CAGE data to ensure a high level of confidence in the methylation level estimates, as per published recommendations (Doherty and Couldrey, 2014; Ziller et al., 2015). This work represents one of the most comprehensive and high-quality methylation profiling datasets in livestock to date. We would expect that reproducible TSS, either annotated or novel, would overlap with hypo-methylated regions of the genome (Yamashita et al., 2005; Yagi et al., 2008). Comparative analysis of the CAGE data with the WGBS methylation levels from eight tissues from Benz2616 was used to investigate methylation levels at the TSS in comparison to gene body and UTR regions. For the majority of genes, the methylation level was much lower around the transcriptionally active TSS or regulatory enhancer candidate regions compared to the gene body (e.g. for gene *IRF2BP2* Figure 7). We overlaid the WGBS hypomethylated regions and the CAGE uni-directional TSS clusters (annotated and 'novel') within 50bp of the promoter. For the eight matching tissues 88.7% of the annotated TSS clusters and 32.2% of the 'novel' TSS were hypomethylated (Figure 8). The combined evidence of the hypomethylation and TSS support the conclusion that 32.2% are in fact novel TSS clusters, whereas 67.8% of the novel TSS clusters lack this confirmation.

bioRxiv preprint doi: https://doi.org/10.1101/2020.07.06.189480; this version posted July 6, 2020. The copyright holder for this preprint (which was not certified by peer review) is the author/funder, who has granted bioRxiv a license to display the preprint in perpetuity. It is made available under aCC-BY-NC-ND 4.0 International license.

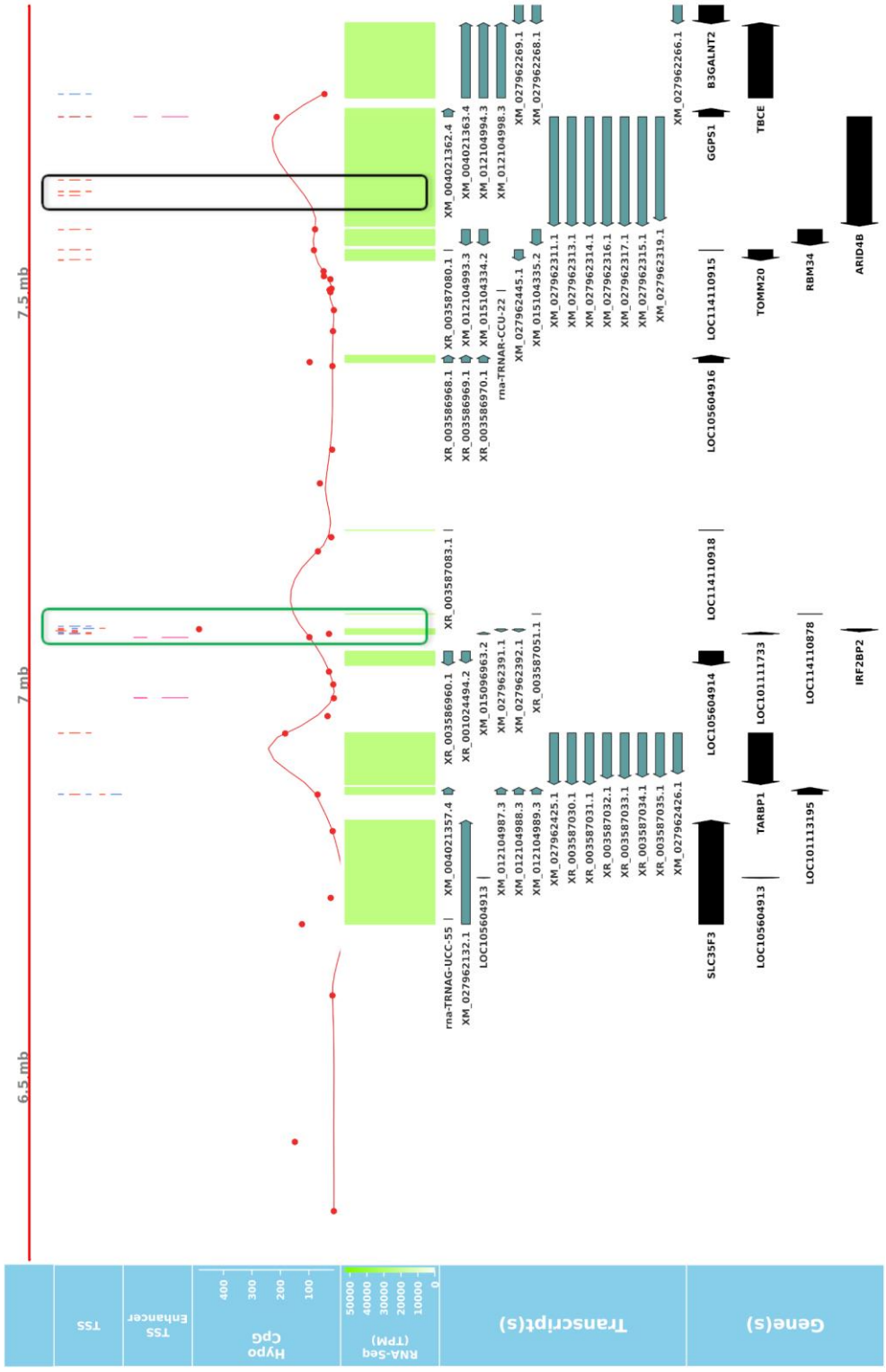

Figure 7. Overlay of CAGE, RNA-Seq and WGBS data tracks centred using the genomic coordinates of gene IRF2BP2. The green box shows a hypomethylated area overlapping multiple uni and bi-directional CAGE tag clusters. The black box represents predicted CAGE tag clusters with no verifying hypomethylation island, which are likely to be 'noise'.

bioRxiv preprint doi: https://doi.org/10.1101/2020.07.06.189480; this version posted July 6, 2020. The copyright holder for this preprint (which was not certified by peer review) is the author/funder, who has granted bioRxiv a license to display the preprint in perpetuity. It is made available under aCC-BY-NC-ND 4.0 International license.

643

A

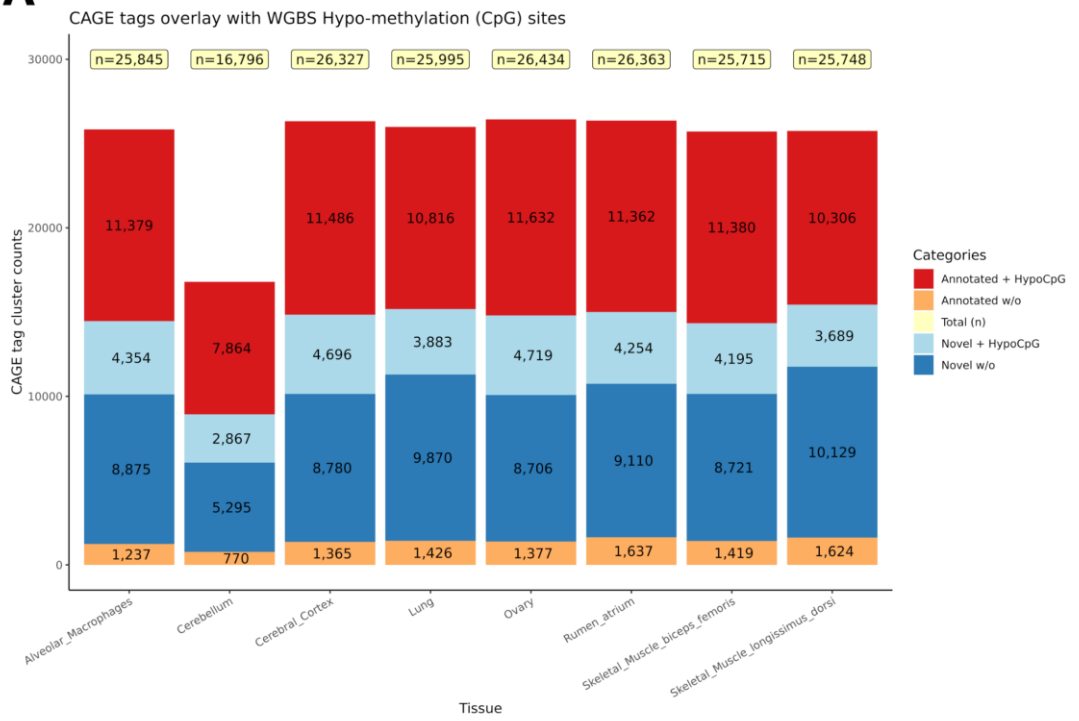

B

Tissue	Annotated + HypoCpG	Annotated w/o	Novel + HypoCpG	Novel w/o
Alveolar_Macrophages	90%	10%	33%	67%
Cerebellum	91%	9%	35%	65%
Cerebral_Cortex	89%	11%	35%	65%
Lung	88%	12%	28%	72%
Ovary	89%	11%	35%	65%
Rumen_atrium	87%	13%	32%	68%
Skeletal_Muscle_biceps_femoris	89%	11%	32%	68%
Skeletal_Muscle_longissimus_dorsi	86%	14%	27%	73%

644

645 *Figure 8: Numbers of CAGE TSS that were hypomethylated according to the WGBS*
646 *data to distinguish between 'novel' reproducible (+HypoCpG) TSS and 'noise' (w/o).*
647 *A) Shows the distribution of CAGE clusters as novel and annotated with or without*
648 *HypoCpG. B) Percentage of CAGE clusters in each categories for each of the eight*
649 *tissues.*

650

651 **Validation of tissue expression profiles using mRNA-Seq**

652 The tissue samples from Benz2616 were collected for the purpose of annotating her
653 genome and as such N=1 in all cases. As an alternative strategy to having multiple
654 biological replicates we validated the expression profiles for each tissue by
655 comparing the CAGE data (CTPM) and mRNA-Seq (TPM) in 52 matching tissues.
656 The transcript expression TPM was significantly correlated with the CAGE tag cluster
657 CTPM values (correlation coefficient 0.19, Pearson *p* value < 1.0e-08) and visualised

bioRxiv preprint doi: https://doi.org/10.1101/2020.07.06.189480; this version posted July 6, 2020. The copyright holder for this preprint (which was not certified by peer review) is the author/funder, who has granted bioRxiv a license to display the preprint in perpetuity. It is made available under aCC-BY-NC-ND 4.0 International license.

as a heatmap (Supplementary Figure S4). A subset of house-keeping transcripts that exhibit consistent expression for both the CAGE and mRNA-Seq datasets across all tissues sampled, are visible from the heatmap (Supplementary Figure S4).

The similarity of tissue expression profiles for the uni-directional TSS clusters was estimated in order to determine if tissues with similar physiology and function formed distinct groups as expected. Similarity (distance) analysis showed a partial grouping based on tissue type and organ system as shown in Figure 9A. Physiologically similar tissues including nervous system and muscle tissues grouped closely together. This grouping was also present in the mRNA-Seq data from tissue matched samples Figure 9B, indicating good correlation between the two datasets.

bioRxiv preprint doi: https://doi.org/10.1101/2020.07.06.189480; this version posted July 6, 2020. The copyright holder for this preprint (which was not certified by peer review) is the author/funder, who has granted bioRxiv a license to display the preprint in perpetuity. It is made available under aCC-BY-NC-ND 4.0 International license.

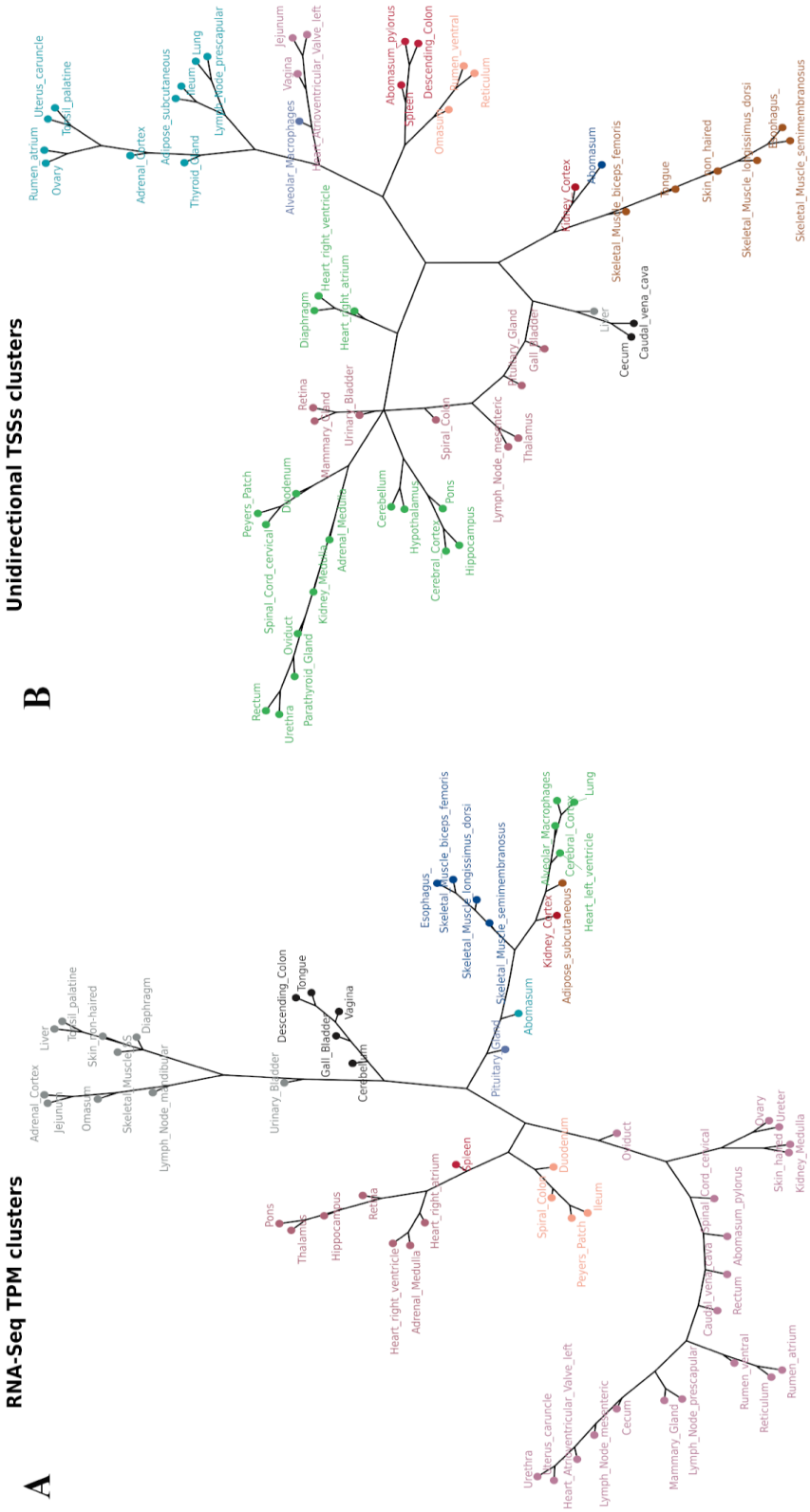

669

670 *Figure 9. The network analysis of tissue TSS and gene expression profiles in 52*
671 *matched samples from Benz1626. The clustering algorithm was based on MI*
672 *distance of each tissue given the expressed A) mRNA-Seq transcript level TPM and*
673 *B) CAGE tag clusters (TSSs).*

bioRxiv preprint doi: https://doi.org/10.1101/2020.07.06.189480; this version posted July 6, 2020. The copyright holder for this preprint (which was not certified by peer review) is the author/funder, who has granted bioRxiv a license to display the preprint in perpetuity. It is made available under aCC-BY-NC-ND 4.0 International license.

674 **Comparative visualisation of the datasets**

675 An interactive visualisation interface was developed in order to make these datasets
676 accessible and useable for the livestock genomics community. The genomic browser
677 incorporates the bp resolution hypomethylation data, the CTPM expression of TSS
678 and TSS-Enhancer regions and the mRNA-Seq TPM expression at transcript level.
679 These tracks are also overlaid using the coordinates provided by the TxDB objects
680 for transcripts and gene models as shown in Figure 10. This form of overlaid view
681 allows for confirmation of transcript expression and the exact coordinate of the
682 corresponding TSS in each tissue. For validation purposes the promoter region
683 should be under a hypo-methylated CpG island on the DNA track for any actively
684 transcribed gene in each tissue. The detailed bigBED format tracks for all the tissues
685 are available at https://data.faang.org/api/fire_api/trackhubregistry/hub.txt.

686 These visualisation tools were used to identify any co-expressed enhancers
687 within the proximity of a TSS. We were able to identify 741 TSS-Enhancer clusters
688 across the 56 tissues. An example of these bi-directional clusters is shown in Figure
689 10 as a pink line. The pairwise CTPM levels of co-expression of the bi-directional
690 clusters and those of the uni-directional TSS clusters were compared using the
691 Kendal correlation function in CAGEfightR (Thodberg and Sandelin, 2019). There
692 were 5383 significant co-expression pairs between uni-directional clusters (28,148)
693 and bi-directional clusters (741). An example of a co-expressed TSS-enhancer is
694 shown in Figure 10 as a black line connecting the significant start positions of the co-
695 expression pairs.

696 The co-expression range of bi-directional clusters, in some cases, can span
697 beyond the 10Kbp distance, as shown in the *IK* gene example Figure 10. The
698 expression of enhancer RNA (eRNA) with the promoter expression level of their
699 target genes has been reported before (Tippens et al., 2018). This layer of annotation
700 provides a foundation for enhancer target mapping in the sheep genome. The
701 detailed list and annotated target transcripts of these co-expression clusters can be
702 found in Supplementary File 2.
703

bioRxiv preprint doi: https://doi.org/10.1101/2020.07.06.189480; this version posted July 6, 2020. The copyright holder for this preprint (which was not certified by peer review) is the author/funder, who has granted bioRxiv a license to display the preprint in perpetuity. It is made available under aCC-BY-NC-ND 4.0 International license.

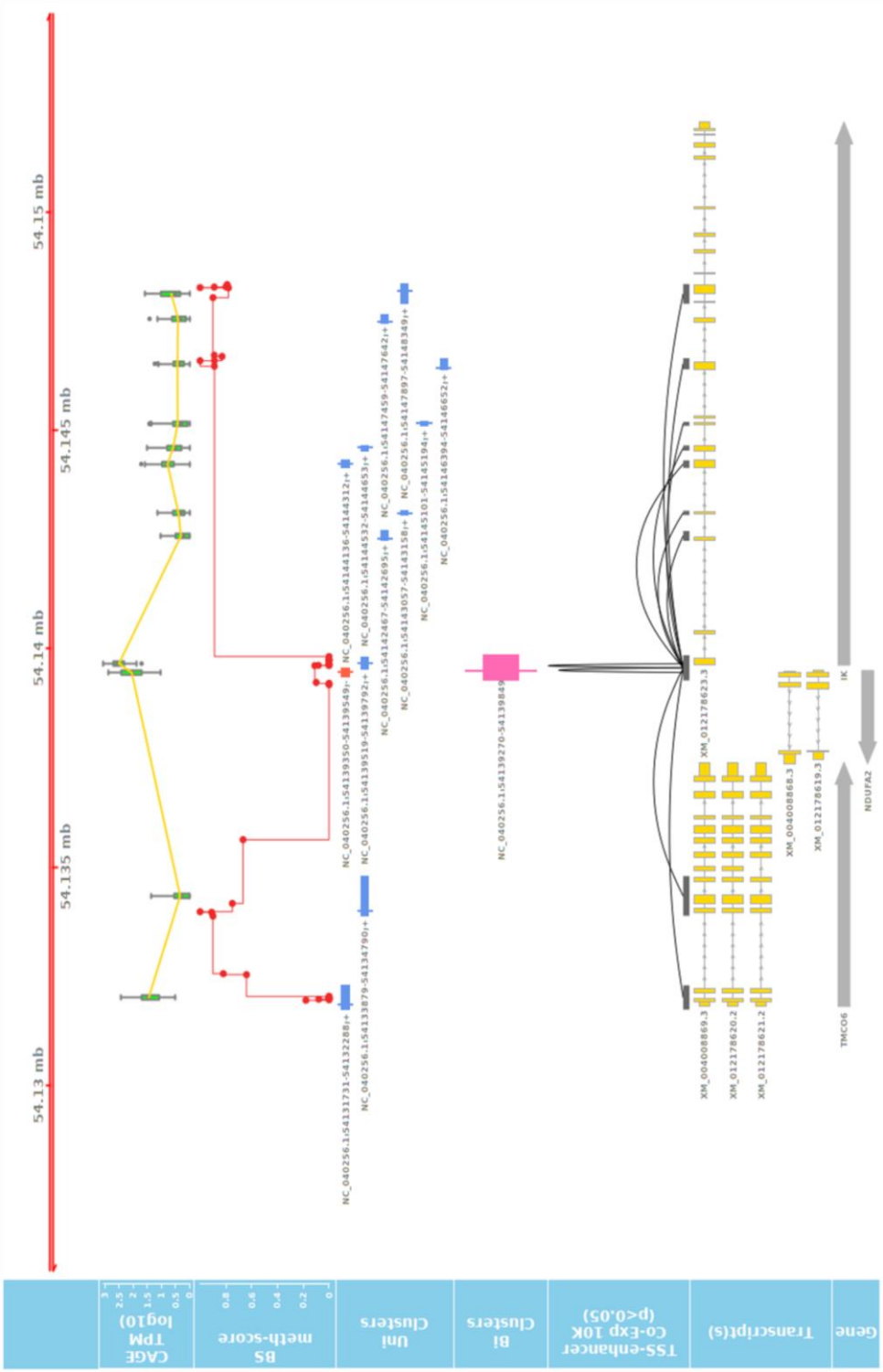

Figure 10. Long range correlation of single enhancer site with multiple promotors of several genes. The track shows the significant correlation of a leading/primary enhancer site highly co-expressed with several TSS sites of different genes in a relatively long coding frame (± 10,000Kb). The 3rd track from the top also shows the level of methylation at CpG sites at DNA level of Benz2616 overlaying the same coordinates of the IK gene and ±10Kbp.

bioRxiv preprint doi: https://doi.org/10.1101/2020.07.06.189480; this version posted July 6, 2020. The copyright holder for this preprint (which was not certified by peer review) is the author/funder, who has granted bioRxiv a license to display the preprint in perpetuity. It is made available under aCC-BY-NC-ND 4.0 International license.

Discussion

High-quality reference genomes are now available for many farmed animal species including domestic sheep (*Ovis aries*). The earlier draft genome sequence (Jiang et al., 2014) has been superseded by a more contiguous genome assembly (*Oar rambouillet v1.0* https://www.ncbi.nlm.nih.gov/assembly/GCF_002742125.1/). Annotation of this genome sequence, however, is currently limited to gene and transcript models. There is a lack of information on regulatory sequences and the complexity of the transcriptome is underestimated. For example, promoters and TSS are not well-annotated and alternative promoters and transcripts are poorly characterised. The overall aim of the Ovine FAANG project was to provide a comprehensive annotation of *Oar rambouillet v1.0*. To contribute to this aim we generated a high-resolution global annotation of transcription start sites (TSS) for sheep. After removal, of CAGE tags with < 10 read counts, 39.3% of TSS overlapped with 5' ends of transcripts, as annotated previously by NCBI. A further 14.7% mapped to within 50bp of annotated promoter regions. Intersecting these predicted TSS regions with annotated promoter regions (±50bp) revealed 46% of the predicted TSS were 'novel' and previously un-annotated. Using whole genome bisulphite sequencing data from the same tissues we were able to determine that a proportion of these 'novel' TSS were hypo-methylated (32.2%) indicating that they are likely to be reproducible rather than 'noise'. This global annotation of TSS in sheep will significantly enhance the annotation of gene models in the new ovine reference assembly (*Oar rambouillet v1.0)*.

The quality of the annotation of reference genomes for livestock species is improving rapidly with reductions in the cost of sequencing and generation of new datasets from multiple different functional assays (Giuffra and Tuggle, 2019). *Oar rambouillet v1.0* superseded the Texel reference assembly (*Oar_v3.1*), which was released in 2014 (Jiang et al., 2014). *Oar_v3.1* is still widely utilised by the sheep genomics community and the Ensembl annotation (https://www.ensembl.org/Ovis_aries/Info/Index) also includes sequence variation information. We compared how mapped CAGE tag clusters were distributed across genomic features in *Oar rambouillet v1.0* and *Oar_v3.1* (Jiang et al., 2014) and found that the proportion of CAGE tag clusters mapping to promoter regions was greater for *Oar rambouillet v1.0* (39%) than *Oar_v3.1* (15%). This may be because *Oar_v3.1* was built using short read technology (Jiang et al., 2014), which had a significant bias to GC rich regions, and therefore did not robustly capture the 5' ends of many genes (Chen et al., 2013). In comparison, the *Oar rambouillet v1.0* assembly was generated

bioRxiv preprint doi: https://doi.org/10.1101/2020.07.06.189480; this version posted July 6, 2020. The copyright holder for this preprint (which was not certified by peer review) is the author/funder, who has granted bioRxiv a license to display the preprint in perpetuity. It is made available under aCC-BY-NC-ND 4.0 International license.

using long read technology, that dramatically improves the ease of assembly resulting in increased contiguity (Contig N50: *Oar_v3.1* 0.07Mb and *Oar rambouillet v1.0* 2.57Mb). Other recent high quality reference genome assemblies for livestock, e.g. goat (Bickhart et al., 2017; Worley, 2017) and water buffalo (Low et al., 2019), have been built using long read sequencing technology in combination with optical mapping for scaffolding.

Highly annotated genomes are powerful tools that can help us to understand the mechanisms underlying complex traits in livestock (Georges et al., 2018; Giuffra and Tuggle, 2019) and mitigate future challenges to food production (Rexroad et al., 2019). GWAS results, for example, can be integrated with functional annotation information to identify causal variants enriched in trait-linked tissues or cell types (reviewed in (Cano-Gamez and Trynka, 2020)). Using enrichment analysis (Finucane et al., 2018) showed that heritable disease associated variants from GWAS were enriched in enhancer regions in relevant tissues and cell types in humans. The TSS and TSS-enhancer clusters identified in this study could be utilised in a similar way for SNP enrichment analysis of GWAS variants in sheep. Using ChIP-Seq data (Naval-Sanchez et al., 2018) found that selective sweeps were significantly enriched for proximal regulatory elements to protein coding genes and genome features associated with active transcription. A high quality set of variants for sheep, generated using whole genome sequencing information for hundreds of animals across multiple breeds, is available through (Sheep Genomes Database, 2020). This dataset could be used to identify functional SNPs enriched in the TSS and TSS-enhancer clusters for multiple tissues and cell types that we have annotated in the *Oar rambouillet v1.0* assembly. High throughput functional screens using gene editing technologies, are now possible to validate these functional variants (reviewed in (Tait-Burkard et al., 2018)). New iPSC lines for livestock species also now offer the potential to do this in relevant cell types (Ogorevc et al., 2016).

Our high-resolution atlas of TSS complements other available large-scale RNA-Seq datasets for sheep e.g. (Clark et al., 2017). The analysis we present here includes tissues representing all major organ systems. However, we were unable to generate CAGE libraries for a small number of difficult to collect or problematic tissues, and as such may have missed transcripts specific to these tissues. We were also only able to generate CAGE libraries from one isolated cell type, alveolar macrophages. As demonstrated by the FANTOM5 (Forrest et al., 2014) and ENCODE (Birney et al., 2007) and FragENCODE (Foissac et al., 2019) projects, including a diversity of immune cell types, in both activated and inactivated states, in future work would capture additional transcriptional diversity. New technologies, such

bioRxiv preprint doi: https://doi.org/10.1101/2020.07.06.189480; this version posted July 6, 2020. The copyright holder for this preprint (which was not certified by peer review) is the author/funder, who has granted bioRxiv a license to display the preprint in perpetuity. It is made available under aCC-BY-NC-ND 4.0 International license.

as single cell sequencing, will allow annotation of cell-specific expressed and regulatory regions of the genome at unprecedented resolution (Papatheodorou et al., 2019). C1 CAGE now offers the opportunity to detect TSS and enhancer activity at single-cell resolution (Kouno et al., 2019).

We have also generated full-length transcript information using the Iso-Seq method, for a small subset of tissues from Benz2616. Integrating mRNA-Seq and Iso-Seq datasets has been used successfully to improve the annotation of the pig genome (Beiki et al., 2019). By merging the Iso-Seq data with the CAGE and mRNA-Seq datasets we will be able to measure differential transcript usage across tissues and improve the resolution of the *Oar rambouillet v1.0* transcriptome further. As such the study we present here represents just the first step in demonstrating the power and utility of the different datasets generated for the Ovine FAANG project, which will provide one of the highest resolution annotations of transcript regulation and diversity in a livestock species to date.

Acknowledgements

The authors would like to thank the Human Genome Sequencing Center staff for the *Oar rambouillet v1.0* reference genome assembly and for long-read and short read mRNA and miRNA sequencing. HGSC contributors include the genome assembly and analysis team of Y. Liu, R.A. Harris, X. Qin, led by K. Worley and production team members including M-C Gingras and L. Perez for RNA and DNA preparation, V. Vee, Y. Han. V. Korchina, S. Dugan-Perez for sequencing, Q. Meng, H. Doddapaneni, M. Wang for library production, the system support and LIMs teams, D. M. Muzny the HGSC Director of Operations, R. A. Gibbs the HGSC Director. We thank S. Sullivan and I. Liachko of Phase Genomics for PGA genome scaffolding.

We would also like to thank William Thompson for isolation of RNA and Jacky Carnahan for isolation of DNA at USMARC. The authors are grateful to Lucas Lefevre, Rachel Young and Heather Finlayson for performing the initial optimisation to establish the CAGE protocol at the Roslin Institute and Sara Clohisey and Lee Murphy for advice on data analysis and assistance in establishing the protocol at the Edinburgh Clinical Research Facility. The authors are also grateful for the support of the FAANG Data Coordination Centre (http://data.faang.org) in the upload and archiving of the sample data and metadata, and hosting of the genome tracks.

Furthermore, we would like to thank the tissue collection design team; Noelle Cockett and Kim Worley, who coordinated the team, James Kijas, Brian Dalrymple, Tracy Hadfield, Kara Thornton, Tom Baldwin, Shuna Jones, Bob Lee, Sue Hauver, Christy Kelley, Jessica Eisenhauer, Mike Heaton, William Thompson, Timothy Smith,

bioRxiv preprint doi: https://doi.org/10.1101/2020.07.06.189480; this version posted July 6, 2020. The copyright holder for this preprint (which was not certified by peer review) is the author/funder, who has granted bioRxiv a license to display the preprint in perpetuity. It is made available under aCC-BY-NC-ND 4.0 International license.

Stephen White, Michelle Mousel, Alisha Massa; Brian Sayre and Brenda Murdoch who all contributed in planning and designing the collection. Additionally, we would like to thank all those that contributed to the FAANG tissue collection at USU: Noelle Cockett, Tracy Hadfield, Tom Baldwin, Rusty Stott, Arnaud Van Wettere, Holly Mason, Jaqueline LaRose, Dave Forrester, Corey Wareham, Sarah Behunin, Kara Thornton, Gordon Hullinger (VMES), Alisha Massa, Maria Herndon, Brenda Murdoch, Brian Sayre, Caylee Birge, Codie Durfee, Michelle R. Mousel, Rachael Christianson, Nicole Ineck, Angie Robinson, Dallin Wengert, Kerry Rood, Erica Moscoso, Rickie Warr, Dustin Kinney, Abbey Benninghoff, Sumira Phatak, Kevin Contreras, Braden Abercrombie, Misha Regouski.

Ethics Statement

All protocols were approved by the animal care and use in accordance with Utah State University. IACUC approval: #2826, expiration date 21st of February 2021.

Data Availability

All the raw sequence data and analysis BAM files for this study are publicly available via the OAR_USU_Benz2616 NCBI BioProject: https://www.ncbi.nlm.nih.gov/bioproject/PRJNA414087 and via the European Nucleotide Archive (ENA): https://www.ebi.ac.uk/ena/browser/view/PRJEB34864 (CAGE), https://www.ebi.ac.uk/ena/data/view/PRJEB35292 (mRNA-Seq) and http://www.ebi.ac.uk/ena/data/view/PRJEB39178 (WGBS). Details of all 100 samples collected from Benz 2616 are included in the BioSamples database under submission GSB-7268, group accession number SAMEG329607 (https://www.ebi.ac.uk/biosamples/samples/SAMEG329607). The datasets are accessible via the FAANG data portal and were submitted according to FAANG sample and experimental metadata requirements (Harrison et al., 2018). Oar rambouillet v1.0 is now available on the Ensembl Rapid Release site https://rapid.ensembl.org/Ovis_aries_rambouillet/Info/Index.

Author Contributions

RC and IG performed CAGE library, optimisation, preparation and sequencing. MS performed all bioinformatic and data analyses, with the exception of the WGBS data, which was analysed by AC. MS and AC generated the GViz tracks. TPLS coordinated generation of the mRNA-Seq data at US-MARC. KCW coordinated generation of the Oar Rambouillet v1.0 reference assembly and mRNA-Seq data at BCM. SMC coordinated the generation and analysis of the WGBS with AC. ELC and

bioRxiv preprint doi: https://doi.org/10.1101/2020.07.06.189480; this version posted July 6, 2020. The copyright holder for this preprint (which was not certified by peer review) is the author/funder, who has granted bioRxiv a license to display the preprint in perpetuity. It is made available under aCC-BY-NC-ND 4.0 International license.

ALA coordinated the CAGE components of the study. NEC and KCW planned and coordinated the sample collection at USU. BMM is coordinator of the Ovine FAANG project with ALA, SNW, BPD, JWK, RB, NEC, SMC, KCW, ELC and TPLS who designed the overall project and acquired the funding to support the work. ELC wrote the manuscript with MS and AC. All authors contributed to editing and approved the final version of the manuscript.

Conflict of Interest

The authors declare that the research was conducted in the absence of any commercial or financial relationships that could be construed as a potential conflict of interest.

Code Availability

All the code base for the analytical pipeline in this study are available at https://msalavat@bitbucket.org/msalavat/rnaseqwrap_public.git for RNA-Seq analysis, https://msalavat@bitbucket.org/msalavat/cagewrap_public.git for the CAGE mapping, annotation and metrics pipeline and https://msalavat@bitbucket.org/caultona/wgbswrap_public.git for WGBS pipeline.

Funding

This work was supported by National Institute of Food and Agriculture, U.S. Department of Agriculture awards USDA-NIFA-2017-67016-26301 and USDA-NIFA-2013-67015-21228. Sample collection was funded by NRSP-8 Sheep Genome Coordinator Funding, Project UTA-1172. ELC, ALA and MS were partially supported by Institute Strategic Program grants awarded to the Roslin Institute 'Farm Animal Genomics' (BBS/E/D/2021550) and 'Prediction of genes and regulatory elements in farm animal genomes' (BBS/E/D/10002070). ELC is supported by a University of Edinburgh Chancellors Fellowship. The Edinburgh Clinical Research Facility is funded by the Wellcome Trust. AC was supported by the University of Otago PhD scholarship and granted the Marjorie McCallum travel award to visit the Roslin Institute, her PhD research is funded by NZ MBIE C10X1906. TPLS was supported by USDA-ARS Project No. 3040-31000-100-00D. The funders had no role in study design, data collection and analysis, decision to publish, or preparation of the manuscript.

Members of the Ovine FAANG Project Consortium (listed by institution)

bioRxiv preprint doi: https://doi.org/10.1101/2020.07.06.189480; this version posted July 6, 2020. The copyright holder for this preprint (which was not certified by peer review) is the author/funder, who has granted bioRxiv a license to display the preprint in perpetuity. It is made available under aCC-BY-NC-ND 4.0 International license.

Brenda Murdoch (University of Idaho)
Kimberly M Davenport (University of Idaho)
Stephen White (USDA, ARS, Washington State University)
Michelle Mousel (USDA, ARS ADRC)
Alisha Massa (Washington State University)
Kim Worley (Baylor College of Medicine)
Alan Archibald (The Roslin Institute, University of Edinburgh)
Emily Clark (The Roslin Institute, University of Edinburgh)
Brian Dalrymple (University of Western Australia)
James Kijas (CSIRO)
Shannon Clarke (AgResearch)
Rudiger Brauning (AgResearch)
Timothy Smith (USDA, ARS MARC)
Tracey Hadfield (Utah State University)
Noelle Cockett (Utah State University)

References

An, X., Ma, H., Han, P., Zhu, C., Cao, B., and Bai, Y. (2018). Genome-wide differences in DNA methylation changes in caprine ovaries between oestrous and dioestrous phases. *J. Anim. Sci. Biotechnol.* doi:10.1186/s40104-018-0301-x.

Andersson, L., Archibald, A. L., Bottema, C. D., Brauning, R., Burgess, S. C., Burt, D. W., et al. (2015). Coordinated international action to accelerate genome-to-phenome with FAANG, the Functional Annotation of Animal Genomes project. *Genome Biol.* 16, 57. doi:10.1186/s13059-015-0622-4.

Andersson, R., Gebhard, C., Miguel-Escalada, I., Hoof, I., Bornholdt, J., Boyd, M., et al. (2014). An atlas of active enhancers across human cell types and tissues. *Nature* 507, 455–461. doi:10.1038/nature12787.

Baillie, J. K., Arner, E., Daub, C., De Hoon, M., Itoh, M., Kawaji, H., et al. (2017). Analysis of the human monocyte-derived macrophage transcriptome and response to lipopolysaccharide provides new insights into genetic aetiology of inflammatory bowel disease. *PLOS Genet.* 13, e1006641.

Beiki, H., Liu, H., Huang, J., Manchanda, N., Nonneman, D., Smith, T. P. L., et al. (2019). Improved annotation of the domestic pig genome through integration of Iso-Seq and RNA-seq data. *BMC Genomics* 20, 344. doi:10.1186/s12864-019-5709-y.

Berger, M. R., Alvarado, R., and Kiss, D. L. (2019). mRNA 5′ ends targeted by

bioRxiv preprint doi: https://doi.org/10.1101/2020.07.06.189480; this version posted July 6, 2020. The copyright holder for this preprint (which was not certified by peer review) is the author/funder, who has granted bioRxiv a license to display the preprint in perpetuity. It is made available under aCC-BY-NC-ND 4.0 International license.

cytoplasmic recapping cluster at CAGE tags and select transcripts are alternatively spliced. *FEBS Lett.* 593, 670–679. doi:10.1002/1873-3468.13349.

Bertin, N., Mendez, M., Hasegawa, A., Lizio, M., Abugessaisa, I., Severin, J., et al. (2017). Linking FANTOM5 CAGE peaks to annotations with CAGEscan. *Sci. Data* 4, 170147. doi:10.1038/sdata.2017.147.

Bickhart, D. M., Rosen, B. D., Koren, S., Sayre, B. L., Hastie, A. R., Chan, S., et al. (2017). Single-molecule sequencing and chromatin conformation capture enable de novo reference assembly of the domestic goat genome. *Nat. Genet.* 49, 643–650. doi:10.1038/ng.3802.

Birney, E., Stamatoyannopoulos, J. A., Dutta, A., Guigó, R., Gingeras, T. R., Margulies, E. H., et al. (2007). Identification and analysis of functional elements in 1% of the human genome by the ENCODE pilot project. *Nature* 447, 799–816. doi:10.1038/nature05874.

Bray, N. L., Pimentel, H., Melsted, P., and Pachter, L. (2016). Near-optimal probabilistic RNA-seq quantification. *Nat. Biotechnol.* 34, 525–527. doi:10.1038/nbt.3519.

Cano-Gamez, E., and Trynka, G. (2020). From GWAS to Function: Using Functional Genomics to Identify the Mechanisms Underlying Complex Diseases. *Front. Genet.* 11, 424.

Chen, Y.-C., Liu, T., Yu, C.-H., Chiang, T.-Y., and Hwang, C.-C. (2013). Effects of GC Bias in Next-Generation-Sequencing Data on De Novo Genome Assembly. *PLoS One* 8, e62856.

Clark, E. L., Bush, S. J., McCulloch, M. E. B., Farquhar, I. L., Young, R., Lefevre, L., et al. (2017). A high resolution atlas of gene expression in the domestic sheep (Ovis aries). *PLOS Genet.* 13, e1006997.

Cordier, G., Cozon, G., Greenland, T., Rocher, F., Guiguen, F., Guerret, S., et al. (1990). In vivo activation of alveolar macrophages in ovine lentivirus infection. *Clin. Immunol. Immunopathol.* 55, 355–367. doi:https://doi.org/10.1016/0090-1229(90)90124-9.

Ding, B., Gentleman, R., and Carey, V. (2012). bioDist: Different distance measures. R package version 1.28.0. Available at: https://www.bioconductor.org/packages/release/bioc/html/bioDist.html.

Doherty, R., and Couldrey, C. (2014). Exploring genome wide bisulfite sequencing for DNA methylation analysis in livestock: A technical assessment. *Front. Genet.* doi:10.3389/fgene.2014.00126.

Edinburgh, U. of (2020). Edinburgh Compute and Data Facility. Available at: https://www.ed.ac.uk/is/research-computing-service [Accessed July 6, 2020].

bioRxiv preprint doi: https://doi.org/10.1101/2020.07.06.189480; this version posted July 6, 2020. The copyright holder for this preprint (which was not certified by peer review) is the author/funder, who has granted bioRxiv a license to display the preprint in perpetuity. It is made available under aCC-BY-NC-ND 4.0 International license.

970 Finucane, H. K., Reshef, Y. A., Anttila, V., Slowikowski, K., Gusev, A., Byrnes, A., et
971 al. (2018). Heritability enrichment of specifically expressed genes identifies
972 disease-relevant tissues and cell types. *Nat. Genet.* 50, 621–629.
973 doi:10.1038/s41588-018-0081-4.
974 Foissac, S., Djebali, S., Munyard, K., Vialaneix, N., Rau, A., Muret, K., et al. (2019).
975 Multi-species annotation of transcriptome and chromatin structure in
976 domesticated animals. *BMC Biol.* 17, 108. doi:10.1186/s12915-019-0726-5.
977 Forrest, A. R. R., Kawaji, H., Rehli, M., Baillie, J. K., De Hoon, M. J. L., Haberle, V.,
978 et al. (2014). A promoter-level mammalian expression atlas. *Nature* 507, 462–
979 470. doi:10.1038/nature13182.
980 Georges, M., Charlier, C., and Hayes, B. (2018). Harnessing genomic information for
981 livestock improvement. *Nat. Rev. Genet.* 20, 1. doi:10.1038/s41576-018-0082-2.
982 Giuffra, E., and Tuggle, C. K. (2019). Functional Annotation of Animal Genomes
983 (FAANG): Current Achievements and Roadmap. *Annu. Rev. Anim. Biosci.* 7,
984 65–88. doi:10.1146/annurev-animal-020518-114913.
985 Guo, W., Zhu, P., Pellegrini, M., Zhang, M. Q., Wang, X., and Ni, Z. (2018).
986 CGmapTools improves the precision of heterozygous SNV calls and supports
987 allele-specific methylation detection and visualization in bisulfite-sequencing
988 data. *Bioinformatics* 34, 381–387. doi:10.1093/bioinformatics/btx595.
989 Hahne, F., and Ivanek, R. (2016). “Visualizing Genomic Data Using Gviz and
990 Bioconductor BT - Statistical Genomics: Methods and Protocols,” in, eds. E.
991 Mathé and S. Davis (New York, NY: Springer New York), 335–351.
992 doi:10.1007/978-1-4939-3578-9_16.
993 Hannon Lab (2017). FASTX-Toolkit FASTQ/A short reads pre-processing tools.
994 Available at: http://hannonlab.cshl.edu/fastx_toolkit/ [Accessed July 6, 2020].
995 Harrison, P. W., Fan, J., Richardson, D., Clarke, L., Zerbino, D., Cochrane, G., et al.
996 (2018). FAANG, establishing metadata standards, validation and best practices
997 for the farmed and companion animal community. *Anim. Genet.* 49, 520–526.
998 doi:10.1111/age.12736.
999 Ibeagha-Awemu, E. M., and Zhao, X. (2015). Epigenetic marks: Regulators of
1000 livestock phenotypes and conceivable sources of missing variation in livestock
1001 improvement programs. *Front. Genet.* doi:10.3389/fgene.2015.00302.
1002 Jiang, Y., Xie, M., Chen, W., Talbot, R., Maddox, J. F., Faraut, T., et al. (2014). The
1003 sheep genome illuminates biology of the rumen and lipid metabolism. *Science*
1004 344, 1168–1173. doi:10.1126/science.1252806.
1005 Joe, H. (1989). Relative Entropy Measures of Multivariate Dependence. *J. Am. Stat.*
1006 *Assoc.* 84, 157–164. doi:10.1080/01621459.1989.10478751.

bioRxiv preprint doi: https://doi.org/10.1101/2020.07.06.189480; this version posted July 6, 2020. The copyright holder for this preprint (which was not certified by peer review) is the author/funder, who has granted bioRxiv a license to display the preprint in perpetuity. It is made available under aCC-BY-NC-ND 4.0 International license.

1007 Jones, P. A. (2012). Functions of DNA methylation: Islands, start sites, gene bodies
1008 and beyond. *Nat. Rev. Genet.* doi:10.1038/nrg3230.
1009 Kent, W. J., Zweig, A. S., Barber, G., Hinrichs, A. S., and Karolchik, D. (2010).
1010 BigWig and BigBed: enabling browsing of large distributed datasets.
1011 *Bioinformatics* 26, 2204–2207. doi:10.1093/bioinformatics/btq351.
1012 Kouno, T., Moody, J., Kwon, A. T.-J., Shibayama, Y., Kato, S., Huang, Y., et al.
1013 (2019). C1 CAGE detects transcription start sites and enhancer activity at
1014 single-cell resolution. *Nat. Commun.* 10, 360. doi:10.1038/s41467-018-08126-5.
1015 Langmead, B., and Salzberg, S. L. (2012). Fast gapped-read alignment with Bowtie
1016 2. *Nat. Methods* 9, 357–359. doi:10.1038/nmeth.1923.
1017 Lassmann, T. (2015). TagDust2: a generic method to extract reads from sequencing
1018 data. *BMC Bioinformatics* 16, 24. doi:10.1186/s12859-015-0454-y.
1019 Lawrence, M., Huber, W., Pagès, H., Aboyoun, P., Carlson, M., Gentleman, R., et al.
1020 (2013). Software for computing and annotating genomic ranges. *PLoS Comput.*
1021 *Biol.* 9, e1003118–e1003118. doi:10.1371/journal.pcbi.1003118.
1022 Lev Maor, G., Yearim, A., and Ast, G. (2015). The alternative role of DNA methylation
1023 in splicing regulation. *Trends Genet.* doi:10.1016/j.tig.2015.03.002.
1024 Li, H., Handsaker, B., Wysoker, A., Fennell, T., Ruan, J., Homer, N., et al. (2009).
1025 The Sequence Alignment/Map format and SAMtools. *Bioinformatics* 25, 2078–
1026 2079. doi:10.1093/bioinformatics/btp352.
1027 Lizio, M., Deviatiiarov, R., Nagai, H., Galan, L., Arner, E., Itoh, M., et al. (2017).
1028 Systematic analysis of transcription start sites in avian development. *PLOS Biol.*
1029 15, e2002887.
1030 Low, W. Y., Tearle, R., Bickhart, D. M., Rosen, B. D., Kingan, S. B., Swale, T., et al.
1031 (2019). Chromosome-level assembly of the water buffalo genome surpasses
1032 human and goat genomes in sequence contiguity. *Nat. Commun.* 10, 260.
1033 doi:10.1038/s41467-018-08260-0.
1034 Murdoch, B. M. (2019). The functional annotation of the sheep genome project. *J.*
1035 *Anim. Sci.* 97, 16.
1036 Naval-Sanchez, M., Nguyen, Q., McWilliam, S., Porto-Neto, L. R., Tellam, R.,
1037 Vuocolo, T., et al. (2018). Sheep genome functional annotation reveals proximal
1038 regulatory elements contributed to the evolution of modern breeds. *Nat.*
1039 *Commun.* 9, 859. doi:10.1038/s41467-017-02809-1.
1040 Ogorevc, J., Orehek, S., and Dovč, P. (2016). Cellular reprogramming in farm
1041 animals: an overview of iPSC generation in the mammalian farm animal
1042 species. *J. Anim. Sci. Biotechnol.* 7, 10. doi:10.1186/s40104-016-0070-3.
1043 Pages, H. (2020). BSgenome: Software infrastructure for efficient representation of

bioRxiv preprint doi: https://doi.org/10.1101/2020.07.06.189480; this version posted July 6, 2020. The copyright holder for this preprint (which was not certified by peer review) is the author/funder, who has granted bioRxiv a license to display the preprint in perpetuity. It is made available under aCC-BY-NC-ND 4.0 International license.

full genomes and their SNPs. R package version 1.56.0.

Papatheodorou, I., Moreno, P., Manning, J., Fuentes, A. M.-P., George, N., Fexova, S., et al. (2019). Expression Atlas update: from tissues to single cells. *Nucleic Acids Res.* 48, D77–D83. doi:10.1093/nar/gkz947.

Priness, I., Maimon, O., and Ben-Gal, I. (2007). Evaluation of gene-expression clustering via mutual information distance measure. *BMC Bioinformatics* 8, 111. doi:10.1186/1471-2105-8-111.

Quinlan, A. R., and Hall, I. M. (2010). BEDTools: A flexible suite of utilities for comparing genomic features. *Bioinformatics* 26, 841–842. doi:10.1093/bioinformatics/btq033.

Reshef, D. N., Reshef, Y. A., Sabeti, P. C., and Mitzenmacher, M. (2018). An empirical study of the maximal and total information coefficients and leading measures of dependence. *Ann. Appl. Stat.* 12, 123–155. doi:10.1214/17-AOAS1093.

Rexroad, C., Vallet, J., Matukumalli, L. K., Reecy, J., Bickhart, D., Blackburn, H., et al. (2019). Genome to Phenome: Improving Animal Health, Production, and Well-Being – A New USDA Blueprint for Animal Genome Research 2018–2027 . *Front. Genet.* 10, 327.

Sheep Genomes Database (2020). Available at: https://sheepgenomesdb.org/ [Accessed July 6, 2020].

Song, Q., Decato, B., Hong, E. E., Zhou, M., Fang, F., Qu, J., et al. (2013). A reference methylome database and analysis pipeline to facilitate integrative and comparative epigenomics. *PLoS One* 8, e81148–e81148. doi:10.1371/journal.pone.0081148.

Tait-Burkard, C., Doeschl-Wilson, A., McGrew, M. J., Archibald, A. L., Sang, H. M., Houston, R. D., et al. (2018). Livestock 2.0 – genome editing for fitter, healthier, and more productive farmed animals. *Genome Biol.* 19, 204. doi:10.1186/s13059-018-1583-1.

Takahashi, H., Kato, S., Murata, M., and Carninci, P. (2012). “CAGE (Cap Analysis of Gene Expression): A Protocol for the Detection of Promoter and Transcriptional Networks,” in *Methods in Molecular Biology*, 181–200. doi:10.1007/978-1-61779-292-2_11.

Thodberg, M., and Sandelin, A. (2019). A step-by-step guide to analyzing CAGE data using R/Bioconductor. *F1000Research* 8, 886. doi:10.12688/f1000research.18456.1.

Thodberg, M., Thieffry, A., Vitting-Seerup, K., Andersson, R., and Sandelin, A. (2019). CAGEfightR: analysis of 5′-end data using R/Bioconductor. *BMC*

bioRxiv preprint doi: https://doi.org/10.1101/2020.07.06.189480; this version posted July 6, 2020. The copyright holder for this preprint (which was not certified by peer review) is the author/funder, who has granted bioRxiv a license to display the preprint in perpetuity. It is made available under aCC-BY-NC-ND 4.0 International license.

Bioinformatics 20, 487. doi:10.1186/s12859-019-3029-5.

Tippens, N. D., Vihervaara, A., and Lis, J. T. (2018). Enhancer transcription: what, where, when, and why? *Genes Dev.* 32, 1–3. doi:10.1101/GAD.311605.118.

Worley, K. C. (2017). A golden goat genome. *Nat. Genet.* 49, 485–486. doi:10.1038/ng.3824.

Yagi, S., Hirabayashi, K., Sato, S., Li, W., Takahashi, Y., Hirakawa, T., et al. (2008). DNA methylation profile of tissue-dependent and differentially methylated regions (T-DMRs) in mouse promoter regions demonstrating tissue-specific gene expression. *Genome Res.* 18, 1969–1978. doi:10.1101/gr.074070.107.

Yamashita, R., Suzuki, Y., Sugano, S., and Nakai, K. (2005). Genome-wide analysis reveals strong correlation between CpG islands with nearby transcription start sites of genes and their tissue specificity. *Gene* 350, 129–136. doi:https://doi.org/10.1016/j.gene.2005.01.012.

Ziller, M. J., Hansen, K. D., Meissner, A., and Aryee, M. J. (2015). Coverage recommendations for methylation analysis by whole-genome bisulfite sequencing. *Nat. Methods*. doi:10.1038/nmeth.3152.

Figure Legends

Figure 1. FAANG assays (CAGE, WGBS and mRNA-Seq) performed on each tissue from Benz2616.

Figure 2. Workflow of the analysis pipeline and respective tools used for CAGE sequence data analysis

Figure 3. Schematic representation of the two clustering algorithms used in the CAGEfightR package for TSS (uni-directional) and TSS-Enhancer (bi-directional) clustering.

Figure 4. The genomic region distribution of CAGE tag clusters mapped against *Oar rambouillet v1.0* assembly and gene annotation. The counts were averaged across tissues. A) Uni-directional TSS clusters with the highest proportion in promoter region (±100bp of the 5'UTR beginning at the [TSS]). B) Bi-directional TSS-enhancer clusters with the highest proportion in the proximal region (1000bp upstream of the 5'UTR beginning at the [TSS]).

bioRxiv preprint doi: https://doi.org/10.1101/2020.07.06.189480; this version posted July 6, 2020. The copyright holder for this preprint (which was not certified by peer review) is the author/funder, who has granted bioRxiv a license to display the preprint in perpetuity. It is made available under aCC-BY-NC-ND 4.0 International license.

Figure 5. Chord diagram of expression level (TPM) of CAGE tag clusters (uni-directional TSS) across all the tissues collected from Benz2616. Shared CAGE tag clusters are common to at least 2/3rd of the tissues (37/56).

Figure 6. Chord diagram of expression level (TPM) of CAGE tag clusters (bi-directional TSS-Enhancer) across all the tissues collected from Benz2616. CAGE tag clusters expressed (>10 CTPM) by at least 2/3rd of the tissues (37/56).

Figure 7. Overlay of CAGE, RNA-Seq and WGBS data tracks centred using the genomic coordinates of gene *IRF2BP2*. The green box shows a hypomethylated area overlapping multiple uni and bi-directional CAGE tag clusters. The black box represents predicted CAGE tag clusters with no verifying hypomethylation island, which are likely to be 'noise'.

Figure 8: Numbers of CAGE TSS that were hypomethylated according to the WGBS data to distinguish between 'novel' reproducible (+HypoCpG) TSS and 'noise' (w/o). A) Shows the distribution of CAGE clusters as novel and annotated with or without HypoCpG. B) Percentage of CAGE clusters in each categories for each of the eight tissues.

Figure 9. The network analysis of tissue TSS and gene expression profiles in 52 matched samples from Benz1626. The clustering algorithm was based on MI distance of each tissue given the expressed A) mRNA-Seq transcript level TPM and B) CAGE tag clusters (TSSs).

Figure 10. Long range correlation of single enhancer site with multiple promotors of several genes. The track shows the significant correlation of a leading/primary enhancer site highly co-expressed with several TSS sites of different genes in a relatively long coding frame (± 10,000Kb). The 3rd track from the top also shows the level of methylation at CpG sites at DNA level of Benz2616 overlaying the same coordinates of the IK gene and ±10Kbp.

bioRxiv preprint doi: https://doi.org/10.1101/2020.07.06.189480; this version posted July 6, 2020. The copyright holder for this preprint (which was not certified by peer review) is the author/funder, who has granted bioRxiv a license to display the preprint in perpetuity. It is made available under aCC-BY-NC-ND 4.0 International license.

Supplemental Material

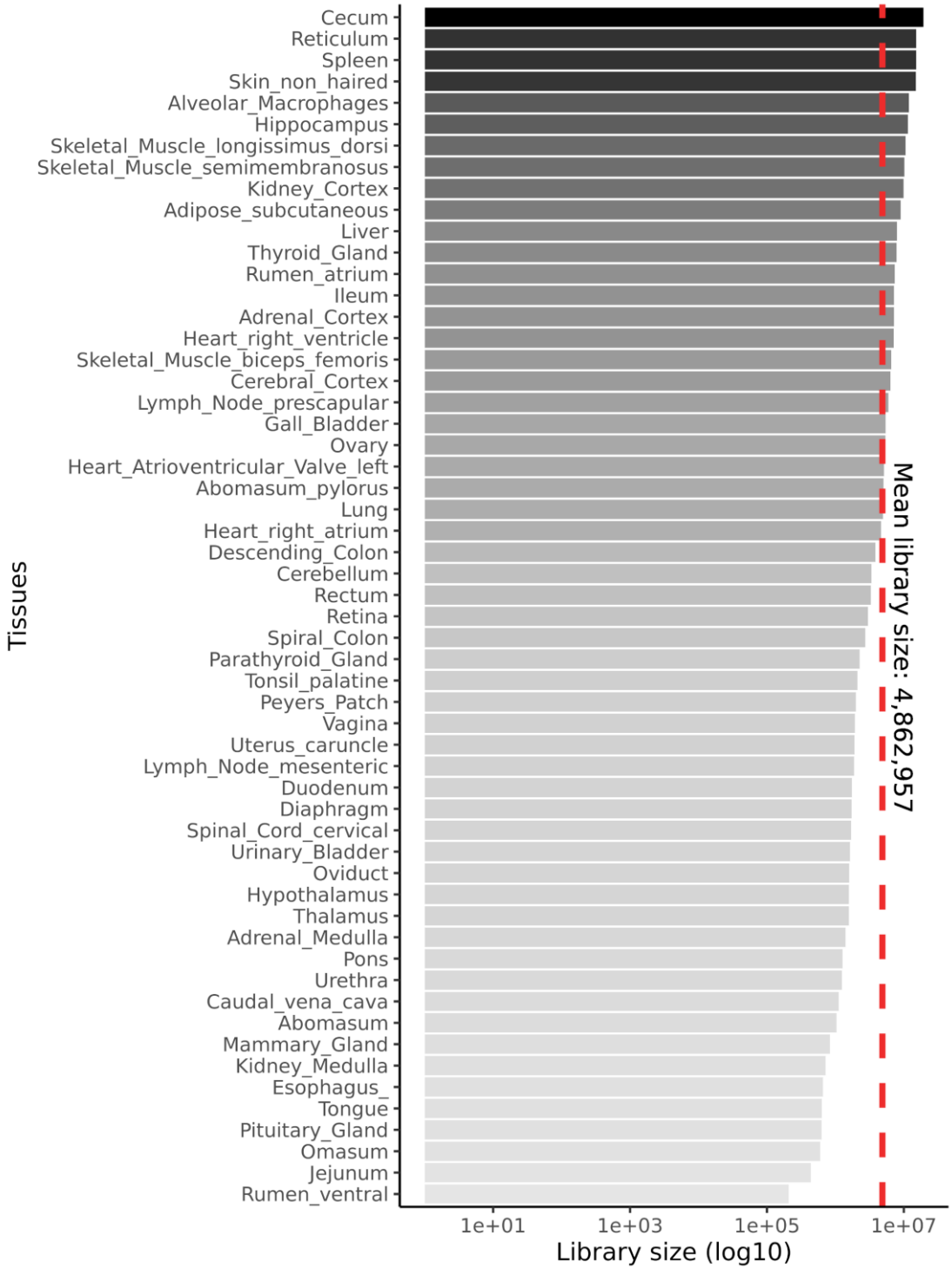

Supplementary Figure S1. CAGE library size for each of the 56 tissues analysed.

bioRxiv preprint doi: https://doi.org/10.1101/2020.07.06.189480; this version posted July 6, 2020. The copyright holder for this preprint (which was not certified by peer review) is the author/funder, who has granted bioRxiv a license to display the preprint in perpetuity. It is made available under aCC-BY-NC-ND 4.0 International license.

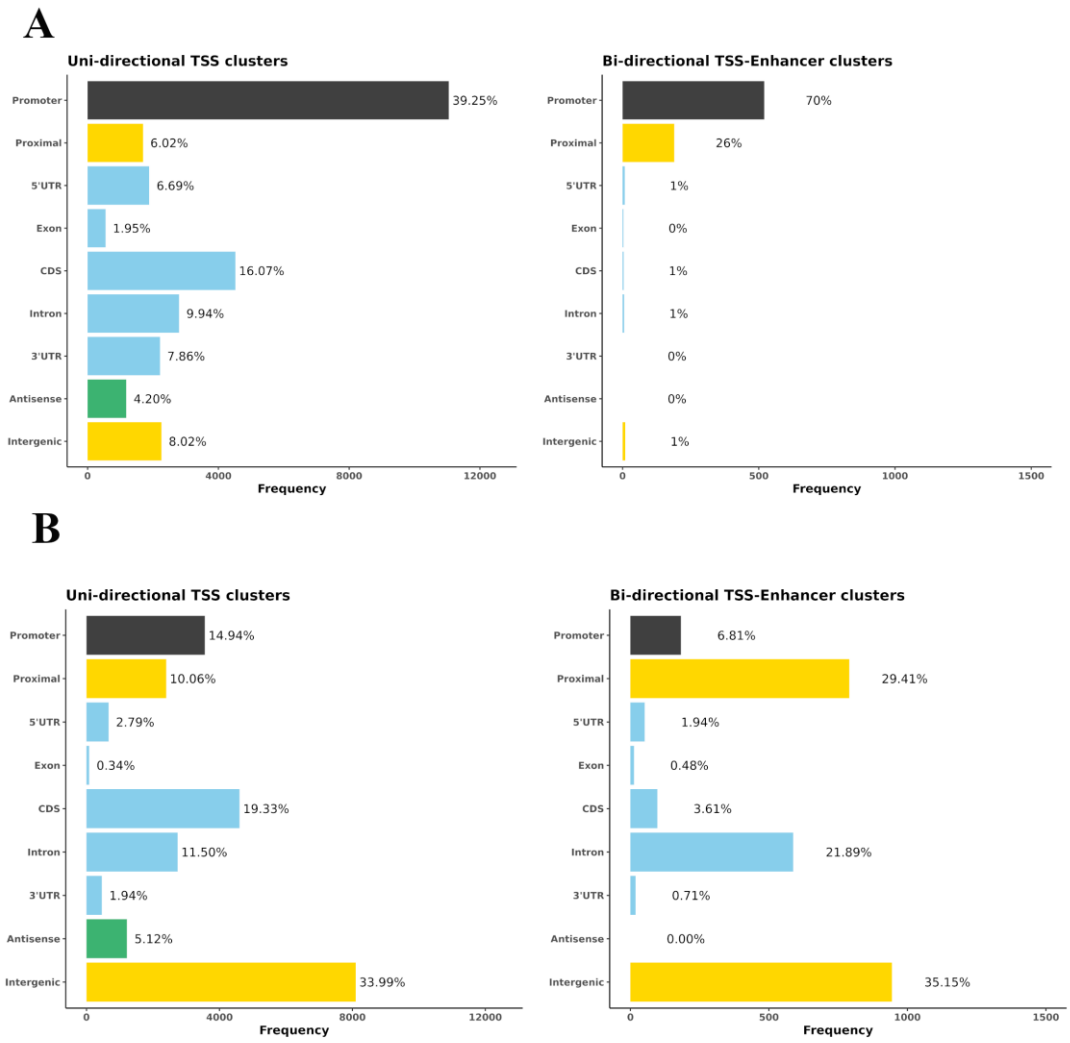

Supplementary Figure S2. The percentage of CAGE tags mapped to each genomic region for Oar_rambouillet_v1.0 (A) and Oar_v3.1 (B) reference genome assemblies. The counts were average across tissues prior to annotation.

bioRxiv preprint doi: https://doi.org/10.1101/2020.07.06.189480; this version posted July 6, 2020. The copyright holder for this preprint (which was not certified by peer review) is the author/funder, who has granted bioRxiv a license to display the preprint in perpetuity. It is made available under aCC-BY-NC-ND 4.0 International license.

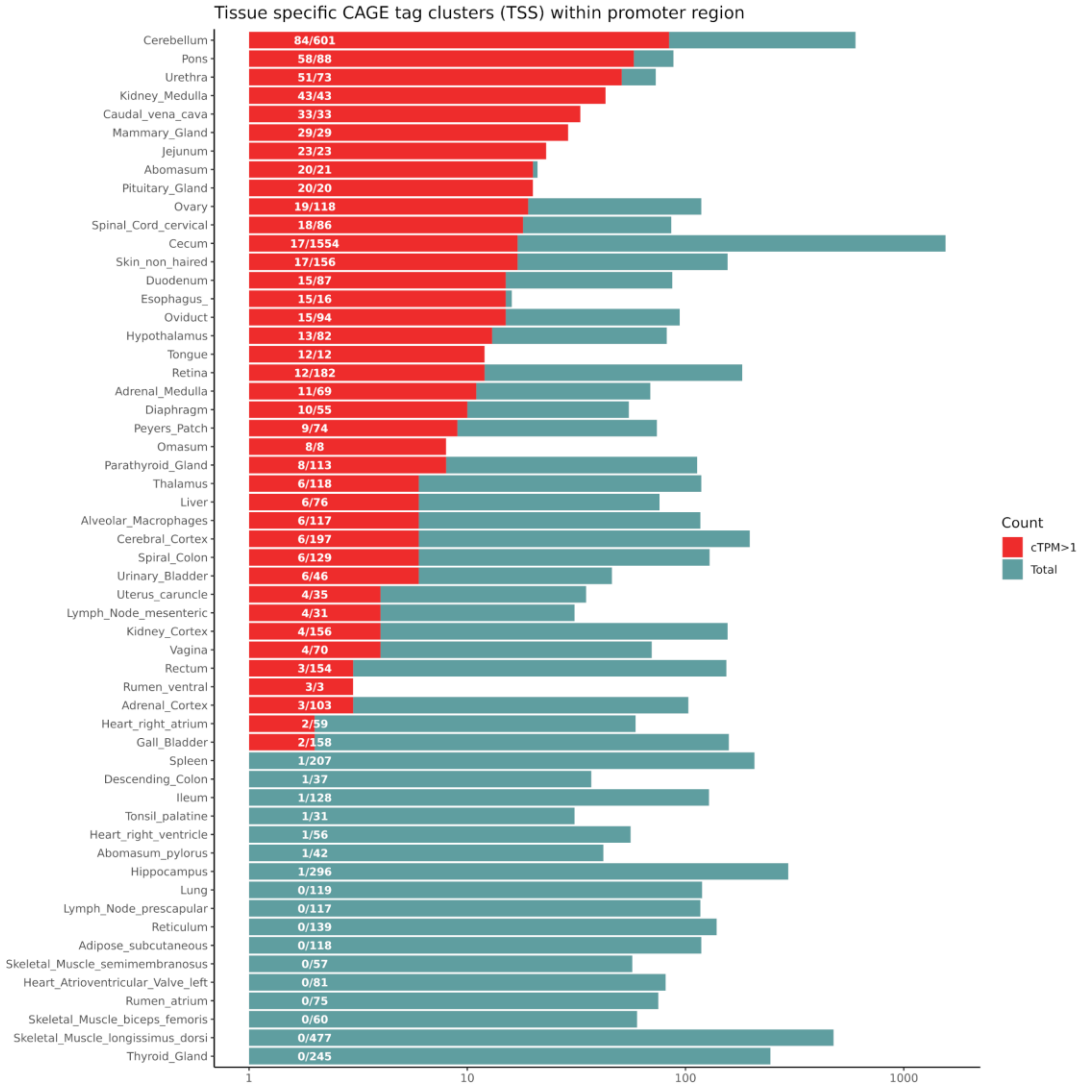

Supplementary Figure S3A. The distribution of tissue specific TSS in 56 tissues of Benz2616. The bar shows the count of tissue specific TSS in each tissue with the proportion being expressed with CTPM >1 coloured in red.

bioRxiv preprint doi: https://doi.org/10.1101/2020.07.06.189480; this version posted July 6, 2020. The copyright holder for this preprint (which was not certified by peer review) is the author/funder, who has granted bioRxiv a license to display the preprint in perpetuity. It is made available under aCC-BY-NC-ND 4.0 International license.

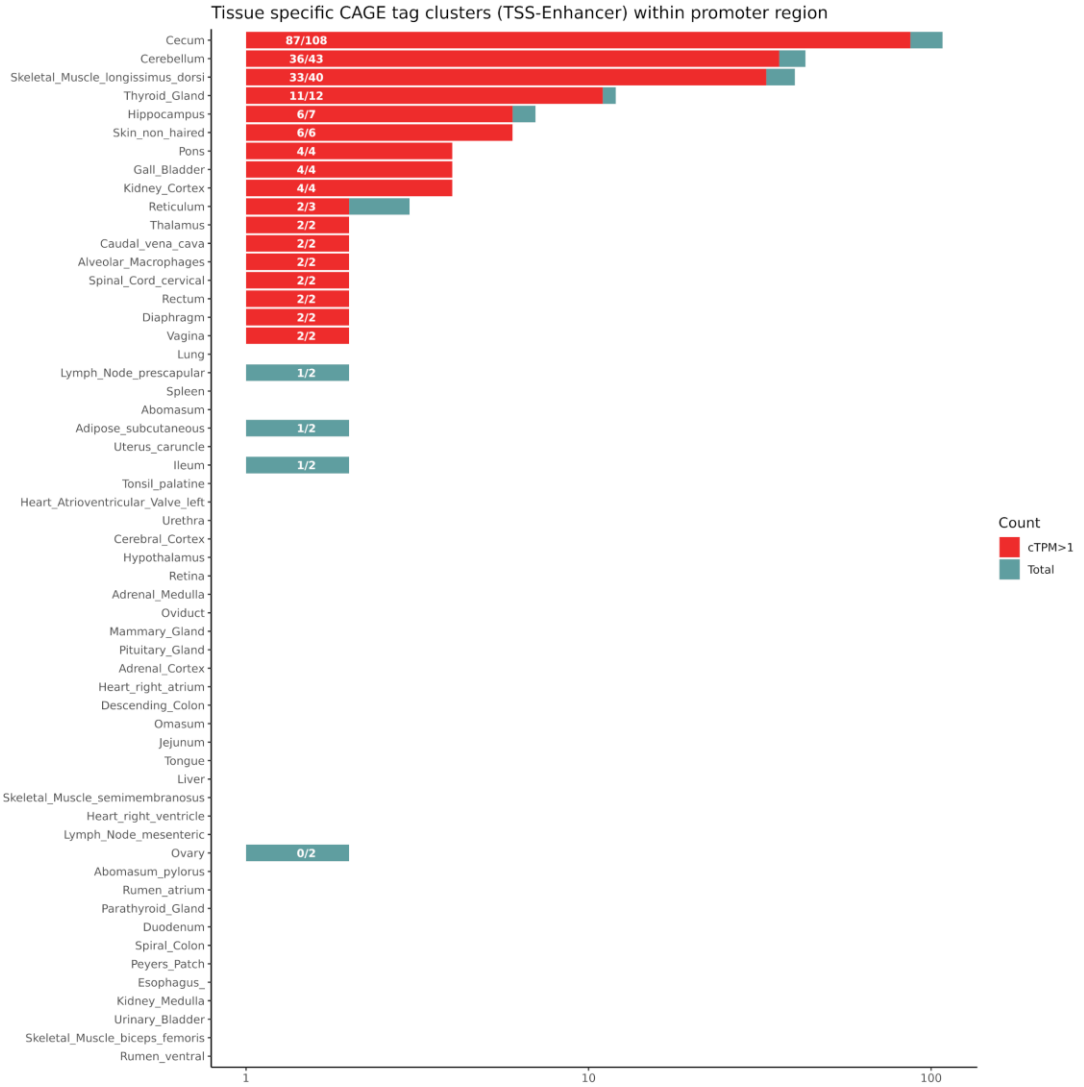

Supplementary Figure S3B. The distribution of tissue specific TSS-Enhancers across the 56 tissues from Benz2616. The bars show the count of tissue specific TSS in each tissue with the proportion being expressed with CTPM >1 coloured in red.

bioRxiv preprint doi: https://doi.org/10.1101/2020.07.06.189480; this version posted July 6, 2020. The copyright holder for this preprint (which was not certified by peer review) is the author/funder, who has granted bioRxiv a license to display the preprint in perpetuity. It is made available under aCC-BY-NC-ND 4.0 International license.

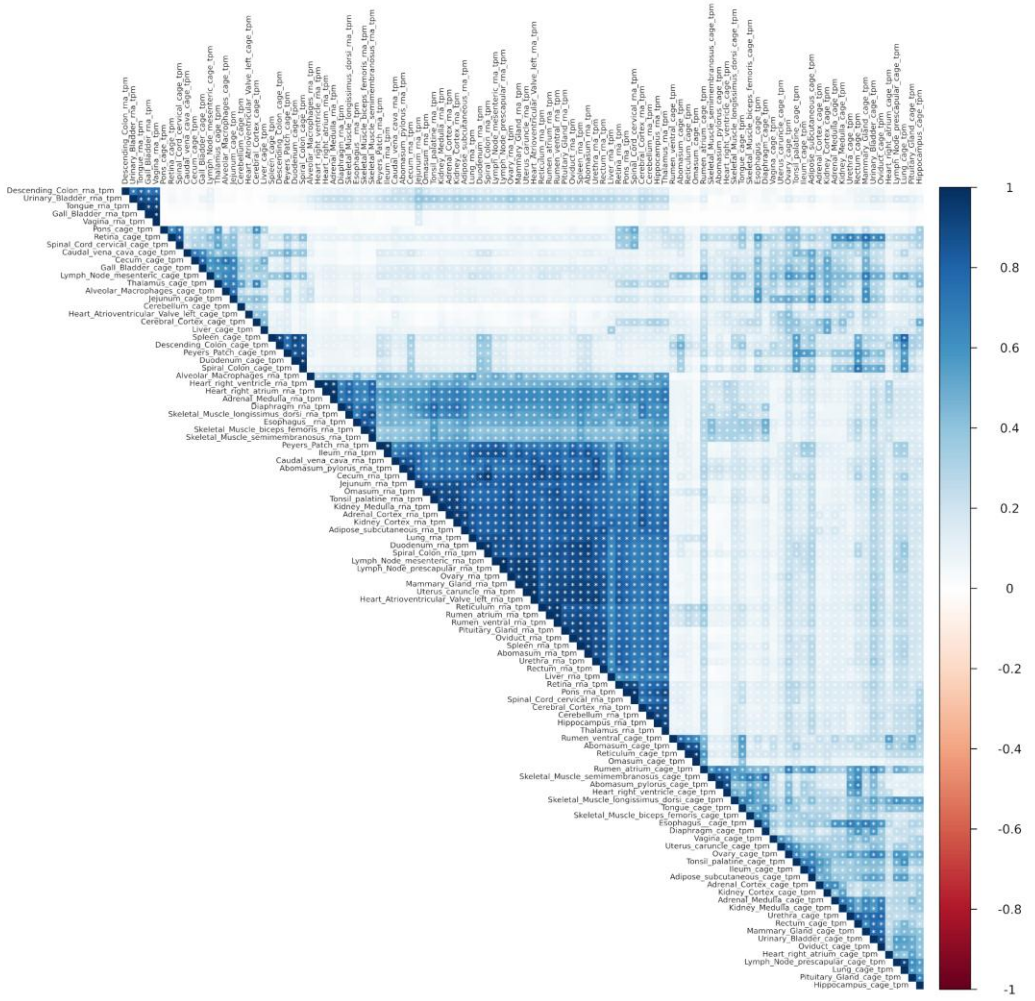

Supplementary Figure S4. Heatmap of mRNA-Seq and CAGE expression profiles (TPM and CTPM). The correlation was calculated over 52 matched tissues and 5732 transcripts-TSS expressed in all tissues.

Supplementary Table 1. Details of 5' linker barcodes and pool ID assigned to each tissue sample.

Supplementary Table 2. Percentage of tissue-specific CAGE tags mapping to genomic features.

Supplementary Table .3. Summary of WGBS sequencing and mapping results.

bioRxiv preprint doi: https://doi.org/10.1101/2020.07.06.189480; this version posted July 6, 2020. The copyright holder for this preprint (which was not certified by peer review) is the author/funder, who has granted bioRxiv a license to display the preprint in perpetuity. It is made available under aCC-BY-NC-ND 4.0 International license.

Supplementary File 1. A detailed comparison of mapping of the CAGE tags to the two reference assemblies Oar_v3.1 and Oar_rambouillet_v1.0 and rational for selecting the 2/3rd representation threshold for mapped CAGE tags.

Supplementary File 2. Expression data frames from Uni-, Bi-directional, long range Linked co-expression clustering and transcript level mRNA-Seq from all 56 tissues (2/3 representation rule applied).